Copyright Warning & Restrictions

The copyright law of the United States (Title 17, United States Code) governs the making of photocopies or other reproductions of copyrighted material.

Under certain conditions specified in the law, libraries and archives are authorized to furnish a photocopy or other reproduction. One of these specified conditions is that the photocopy or reproduction is not to be "used for any purpose other than private study, scholarship, or research." If a, user makes a request for, or later uses, a photocopy or reproduction for purposes in excess of "fair use" that user may be liable for copyright infringement,

This institution reserves the right to refuse to accept a copying order if, in its judgment, fulfillment of the order would involve violation of copyright law.

Please Note: The author retains the copyright while the New Jersey Institute of Technology reserves the right to distribute this thesis or dissertation

Printing note: If you do not wish to print this page, then select "Pages from: first page # to: last page #" on the print dialog screen

HEAT TRANSFER CHARACTERISTICS

OF

NON-NEWTONIAN SUSPENSIONS

A THESIS
SUBMITTED TO THE FACULTY OF
THE DEPARTMENT OF CHEMICAL ENGINEERING
OF
NEWARK COLLEGE OF ENGINEERING

BY

ROBERT G. QUINN, B.S.

IN PARTIAL FULFILLMENT OF THE REQUIREMENTS
FOR THE DEGREE OF

MASTER OF SCIENCE
IN CHEMICAL ENGINEERING

AND

IRVING BAUMAN, B.S.

IN PARTIAL FULFILLMENT OF THE REQUIREMENTS
FOR THE DEGREE OF

MASTER OF SCIENCE
WITH A MAJOR IN CHEMICAL ENGINEERING

NEWARK, NEW JERSEY

1954

APPROVAL OF THESIS

FOR

DEPARTMENT OF CHEMICAL ENGINEERING

NEWARK COLLEGE OF ENGINEERING

BY

FACULTY COMMITTEE

APPROVED: _____

_____

_____

NEWARK, NEW JERSEY

June, 1954

TABLE OF CONTENTS

TABLE OF CONTENTS

LIST OF FIGURES

ACKNOWLEDGMENTS

The authors express their sincere appreciation to Dr. Jerome J. Salamone for his assistance, confidence, interest and guidance in carrying this project to a successful conclusion.

The authors gratefully acknowledge the sincere efforts of Mr. William Furmadge who assisted in the construction of the elaborate apparatus required for the work herein described.

The authors wish to acknowledge their collaborators in this work, Mr. Harold Binder and Mr. Paul Pollara, who shared in the work of constructing the apparatus and collecting the necessary data.

ABSTRACT

This project was undertaken to collect additional information on the heat transfer coefficients of pseudo-plastic suspensions and to test the exponents of the equation of Salamone (12). Using the same equation as derived by Salamone by dimensional analysis, a better correlation of this data was obtained by changing some of the exponents to give the following equation:

$$\frac{hD}{k_f} = 0.346 \left(\frac{Dv\rho}{\mu'}\right)^{0.7} \left(\frac{C_f \mu'}{k_f}\right)^{0.72} \left(\frac{D_s}{D}\right)^{0.15} \left(\frac{C_s}{C_f}\right)^{0.35} \left(\frac{k_s}{k_f}\right)^{0.08} \quad (1)$$

The authors believe that a better correlation is possible and that additional data should be collected on a greater variety of solids in suspension over a large range of Reynolds Numbers.

INTRODUCTION

The object of this research was to check an equation developed by J. J. Salamone (12) for predicting the film coefficient of heat transfer for non-Newtonian suspensions in turbulent flow. His investigation was prompted by the lack of such an equation and by the hypothesis gained from fragmentary data that suspensions of finely divided solid particles of high thermal conductivities in a liquid medium would improve the heat transfer properties of the liquid.

The equation referred to above was developed from data collected in the 50,000 -- 200,000 Reynolds Number range. In the present investigation it was decided to collect data in the 10,000 -- 70,000 Reynolds Number range and from that data re-calculate several of the exponents of the original equation to obtain a check of the equation over the lower turbulent flow region.

The equation referenced above was developed by dimensional analysis, taking into account all of the known variables except particle shape. Another approach (12) was based on the assumption that the existing equation for water could be applied to suspensions provided all the variables introduced by the dispersed phase were included. It was found that all the properties except the bulk viscosity and the effective thermal conductivity of the suspension could be measured or found in the literature. The effective thermal conductivity and the bulk viscosity were determined by calibrating the experimental apparatus with water. The investigation showed that above a Reynolds Number of

50,000 the effective thermal conductivity for each suspension reached some limiting value that was greater than that of the dispersion medium. From the limiting value a linear equation was written. The effective thermal conductivities calculated by Salamone were found to be applicable to the Dittus-Boelter Equation.

This thesis of Bauman and Quinn is one of two which ran concurrently with that of Binder and Pollara. It was the purpose of this half of the work to determine the exponent of the Reynolds Number and of the particle size expression (D/D_s). Binder and Pollara investigated the exponent of the expression (Ks/Kf) and compared the correlation of Salamone to this new correlation using the new exponents. The data and figures of both halves of this work are shown in each thesis for the convenience of the reader.

THEORY

The newest formula for predicting the coefficient of heat transfer (h) to non-Newtonian solutions of the pseudo-plastic type was developed theoretically by J. J. Salamone -- through the use of dimensional analysis. He concluded that the film coefficient of heat transfer should be a function of:

pipe diameter - D

weight fraction of solid - X

thermal conductivity of the dispersion medium - K_f

average particle diameter - D_s

particle shape

specific heat of solid - C_s

specific heat of dispersion medium - C_f

density of solid - ρ_s

density of dispersion medium - ρ_l

apparent bulk viscosity of the suspension - μ_b

velocity, based on bulk density - V_b

Assuming spherical particles and incorporating density of the solid, of the dispersion medium, and weight fraction of solid into a bulk density of the suspension, ρ_b , then by dimensional analysis, the following equation was derived:

$$\frac{h D}{\mu_b C_f} = Z\left(\frac{D V_b \rho_b}{\mu_b}\right)^{\alpha}\left(\frac{k_f}{\mu_b C_f}\right)^{\beta}\left(\frac{k_s}{\mu_b C_f}\right)^{\gamma}\left(\frac{D_s}{D}\right)^{\delta}\left(\frac{C_s}{C_f}\right)^{\phi} \qquad (2)$$

The constants in equation 2 were then determined from experimental data and yielded the following form of the equation:

$$\frac{hD}{\mu_b C_f} = 0.131 \left(\frac{D v_r \rho_r}{\mu_r}\right)^{0.62} \left(\frac{k_f}{\mu_r C_f}\right)^{0.23} \left(\frac{K_s}{\mu_r C_f}\right)^{0.05} \left(\frac{D}{D_s}\right)^{0.05} \left(\frac{C_s}{C_f}\right)^{0.35} \quad (3)$$

Multiply both sides by $\left(\frac{\mu_r C_f}{k_f}\right)$ and rearranging gives:

$$\frac{hD}{k_f} = 0.131 \left(\frac{D v_r \rho_r}{\mu_r}\right)^{0.62} \left(\frac{D}{D_s}\right)^{0.05} \left(\frac{C_s}{C_f}\right)^{0.35} \left(\frac{C_f \mu_r}{k_f}\right)^{0.72} \left(\frac{K_s}{k_f}\right)^{0.05} \quad (4)$$

From inspection of the above equation, it can be seen that variations in μ_b greatly effect the size of the heat transfer coefficient (h). The value of μ_b depends upon the type of suspension used.

Fluids have been found to fall into two general categories, Newtonian and non-Newtonian. A plot of shearing stress versus time rate of shearing strain gives a straight line through the origin for Newtonian fluids. The viscosity is equal to the slope of this line and is constant for any one temperature and pressure.

For a non-Newtonian fluid, the ratio of stress to strain is a function of the time rate of shearing strain, and the apparent viscosity, therefore, depends upon the rate of flow.

The flow of suspensions has been shown by previous investigators to be non-Newtonian and that many are of the pseudo-plastic type where the apparent viscosity decreases with increasing velocity. Data for the stress strain curve for determining the apparent viscosity

may best be obtained from a pipe line viscometer.

These viscosities are based on the fanning friction equation:

$$\frac{\Delta P}{\rho} = f \frac{L}{D} \frac{v^2}{2g_c} \qquad (5)$$

using pressure drop data of the slurry. In order to use the pressure drop data from the viscometer, it is first calibrated with a Newtonian fluid whose density and viscosity is known and a plot of friction factor (f) versus Reynolds Number (Re) made from this experimental data. Then by calculating a friction factor using the bulk density and pressure drop of the slurry, a corresponding Reynolds Number can be found and the bulk viscosity calculated.

From the above, it logically follows that the pipe line viscosity for slurries determined under the same conditions that the heat transfer data was obtained, is the one that should be used for correlating that data.

This is especially true in the case of pseudo-plastics where the viscosity decreases with increase velocity until it reaches some limiting value at complete turbulence where its viscosity is still greater than that of the dispersion medium.

LITERATURE SEARCH

A search was made into the available literature to determine the extent of the work performed by other investigators, to obtain sufficient background for designing the apparatus required, and to organize the experimental work to obtain sufficient data for use in arriving at valid conclusions.

The first engineering investigations on the flow behavior of non-Newtonian fluids in conduits appeared in the work of Wilhelm, Wroughton, and Loeffel (3) at Princeton University and Caldwell and Babbitt (4) at the University of Illinois. The purpose of this work deals primarily with the determination of a procedure for correlating pressure drops for various suspensions. Heretofore, only qualitative information based on minor experimental data had been available. Babbitt and Caldwell used sewage sludge and aqueous suspensions of clay, sand and wood pulp, considering sewage sludge and clay slurries as true plastics. The coefficient of rigidity and the yield value of a sludge were found to be independent of the velocity of flow and the pipe dimensions, but dependent upon the concentration of suspended material, size and character of this material, nature of the continuous phase, temperature, slippage and seepage, gas content and agitation. Their data showed that for a given concentration of suspension, the finer the particle size, the greater the resistance to flow. Agitation was shown to have a definite effect on flow characteristics by a change in particle size and distribution. Density was shown to

be unimportant in the laminar or streamline flow region, but of definite effect on the friction factor above the critical velocity which is that velocity below which the friction loss follows the plastic flow equations of Bingham (5) and above which the friction loss is directly proportional to some power of the velocity between 1.7 and 2.0. Their data on suspensions of clay and sewage sludge indicate in the turbulent flow region that the conventional Reynolds Number vs. friction factor plot, is valid if the viscosity of the dispersion medium is used. The yield value and the rigidity coefficient have no effect on the friction factor in the turbulent region as measured by pressure drop in known sizes and lengths of pipe. This is so, since, in turbulent flow the friction loss is due to impact kinetic energy loss which in turn depends only on the density of the material flowing and its velocity; or, suspended material affects the density but not the viscosity in the turbulent region.

Wilhelm, et al. (3) employed water suspensions of cement rock and Filter-Cel, varying in concentration from 54 to 62% and 21 to 34% solids respectively, and ran them simultaneously in a modified Stormer Viscosimeter (10), and in pressure drop sections of known pipe size and length. For cement rock suspensions pronounced deviations from Newtonian properties were found at low rates of shear (fluid velocity in pipe sections, and RPM in viscosimeter), while at high velocities the suspensions behaved similar to a liquid more viscous than water, Filter-Cel slurries more closely resembled a true fluid of greater viscosity than water. For both cases viscosity

increased with concentration. The pressure drop data obtained could be correlated on the conventional friction factor plot, if a corrected viscosity was employed. This corrected value, which might be referred to as the turbulent viscosity as proposed by Binder and Busher (6), was obtained from a plot of Log Z vs. the RPM of the viscosimeter by extrapolating the straight line obtained to zero shear, or RPM. Log Z is defined as the viscosity that a true fluid would have for the same friction factor as a non-Newtonian fluid where the friction factor is defined for the viscosimeter as the torque divided by the specific gravity and the square of the RPM, and the Reynolds Number as RPM times the specific gravity divided by Z.

Two additional papers have appeared, one on true plastic and the other on pseudo-plastic fluids which substantiate the data of Wilhelm and his workers. Binder and Busher (6) used suspensions of grain in water and prepared data which indicated that, for true plastics, data can be correlated in the turbulent region by an equivalent, or turbulent viscosity which is the viscosity of a true fluid having the same friction factor as the plastic for flow through pipes. The parts of a paper by Winding, et al. (7) on the flow of rubber latexes gives the first data on the flow properties of pseudo-plastics. Here the data obtained in the turbulent region could be properly correlated on the usual friction factor plot by using the viscosity at infinite shear, or the slope of the asymptotic limit of the shear stress, rate of shear diagram for a pseudo-plastic in the laminar flow region.

Based on this work, MacLaren and Stairs (8) measured the vis-

cosity of the Filter-Cel suspensions investigated in (7) by measuring the pressure drop in known sizes and lengths of pipe. By comparing the values thus obtained for Filter-Cel to those for water in the same pipes, it became possible to obtain a value of the viscosity similar to the turbulent viscosity defined by Binder and Busher (6).

In 1949, G.E. Alves (9) presented a summary of much of the available knowledge on the Flow of Non-Newtonian Suspensions. Shear diagrams for several types of Newtonian and Non-Newtonian suspensions flowing in pipe are presented as well as a number of references to the work of the more significant investigators in the field.

The available information on heat transfer to suspensions of solids in liquids is rather limited. Heat transfer coefficients of dilute suspensions of Filter-Cel in a concentric pipe heat exchanger were investigated by MacLaren and Stairs (8). The conductivity of the suspending material, in their case, water, was used to correlate their data and the specific heat calculated on a weight fraction basis. Apparent viscosities in the turbulent range were calculated from the pressure drops in a straight length of pipe. In correlating their data, MacLaren and Stairs found that the points obtained at the high Reynolds Numbers, agreed closely with the correlation for water alone. At low Reynolds Numbers, the points for the slurry and water diverged. At Reynolds Numbers lower than 40,000, it was found that a film of the Filter-Cel was baked on the heating surface. At the higher flow velocities, the slurry moved through the heating section

fast enough to avoid the formation of a deposit.

Hoopes' (11) data on the cooling of 0 - 21% Filter-Cel slurries were found to agree within 10% with the Dittus-Boelter equation with the 0.4 exponent for the Prandtl Number. For the data of MacLaren and Stairs on the same slurries, the Reynolds Number exponent of the Dittus Boelter equation had to be changed from 0.8 to 0.705 and the constant from 0.0225 to 0.0385. Both Hoopes, et al. and MacLaren and Stairs present their slurries as showing Bingham body flow, though MacLaren and Stairs did notice some manifestation of variation of this behavior at low fluid flow rates.

Shandling (10) investigated the heat transfer coefficients to aluminum-water slurries. Like the previously referenced investigator (8), he obtained his data in a steam jacketed heat exchanger which was a component part of a recirculating system. Concentrations of slurry varied from 0.8% to 7.4%; the Reynolds Numbers ranged from 20,000 to 100,000. It was determined that the heat transfer coefficients were not significantly affected with increase in the suspension concentration. A rise in viscosity at low velocities and higher concentrations was found to offset increases in the slurry conductivity. No correlation of the heat transfer coefficients of the suspensions could be made because of particle characteristics which could not be determined. Correlation of $Nu/Pr^{0.4}$ vs. $Re^{.7}$ as indicated by the Dittus Boelter equation gave a series of parallel lines having different ordinate intercepts. The same slope as the line for water data, i.e., 0.7 was obtained.

Bonilla, et al., (15) investigated the heat transfer properties of chalk-water slurries at different concentrations. They found that the cooling of 0 to 21% slurries agrees within 10% with the Dittus-Boelter equation:

$$(hD/k_o) = 0.023(DG/\mu)^{0.8} \quad (C\mu/k_o)^{0.4} \qquad (6)$$

over a Reynolds Number range of 3,000 to 230,000. Best agreement was obtained by using the following values: for k, the thermal conductivity of water; for C, the computed additive specific heat of the slurry; and for μ, the viscosity of the slurry as measured in the Wilhelm and Wroughten viscometer. A correlation between viscosities of the slurry and water was made with the Hatschek equation:

$$\mu_b = \mu_w / 1 - \phi^{1/3}$$

where μ_b = bulk viscosity of slurry

μ_w = viscosity of water

ϕ = volume fraction of solid in suspension

With the properties of the system evaluated in the above manner, the Reynolds, Prandtl and Nusselt Numbers were determined. After plotting $Nu/Pr^{1/3}$ vs. Re, with % solid as a parameter, it was shown that the $Nu/Pr^{1/3}$ value varied inversely with concentration of solid and that the effect was more apparent in the lower Reynolds Number range. The decrease in $Nu/Pr^{1/3}$ was found to be approximately a linear function of the solid concentration in the suspension.

Salamone (12) in 1954 completed a series of experiments with a

number of suspensions consisting of various powdered solids in water. In this investigation, the variables investigated are the individual properties of the suspension's components with the exception of viscosity, velocity, and density which are measured as bulk properties based upon the conditions of heat transfer. The experimental data is correlated by dimensional analysis yielding an exponential relation between the variables assembled in the form of dimensionless groups as given in equations (3) and (4). The results of the experimental data provide the values of the exponents. Another correlation assumes that existing relationships for liquids apply to suspensions, providing that the pertinent properties may be evaluated for the suspension. Evaluation of all properties except the effective thermal conductivity of the suspension could be made. Calibration of the experimental equipment with water resulted in a calculation of the effective thermal conductivity of the suspension. The latter was then correlated with the thermal conductivities of the solid, the liquid and the concentration and particle size of the solid. This investigator chose the turbulent flow region for his work to develop high coefficients of heat transfer and to minimize the problem of settling of the solid particles in the piping system.

Orr and Dallavalle (17) worked with various suspensions of powdered solids in water and ethylene glycol. The equation,

$$\mu_b = \frac{\mu}{\left(1 - \frac{\phi}{\phi'}\right)^{1.8}} \qquad (7)$$

was used to calculate the suspension viscosity. ϕ' is the volume

fraction of the solid in a sedimented bed. Experimental measurements with a Saybolt Type viscosimeter gave results which agreed closely with the above referenced equation. Calculation of the thermal conductivities of the suspensions, using the thermal analogy of the Maxwell relation for the electrical situation, agreed rather well with the conductivities determined experimentally. The data outlined were correlated rather well with the use of the Dittus-Boelter equation as modified by Sieder and Tate (21):

$$\frac{hD}{k} = 0.027 \left(\frac{Dv\rho}{\mu}\right)^{0.8} \left(\frac{C\,\mu}{k}\right)^{1/3} \left(\frac{\mu}{\mu_w}\right)^{0.14} \qquad (8)$$

Heat transfer characteristics of non-Newtonian fluids (single fluid phase) were investigated by Chu, et al. (18). Heat transfer correlations for ordinary liquids were found to apply as long as the proper viscosity and thermal conductivity were used for the solution.

DESCRIPTION OF APPARATUS

A schematic diagram of the apparatus is shown in Figure 1 and photographs of the apparatus are illustrated in Figures 2 and 3. It is very similar to that used in the work of Bonilla (15) and Salamone (12).

The slurry was prepared in a fifty-five gallon open top steel drum provided with a "Lightning" motor driven agitator. A Worthington pump of adequate capacity, driven by a 1½ H.P., 220 volt, 60 cycle, A.C. 3450 RPM motor forced the slurry through the system and back to the tank. A by-pass was installed to insure positive rate control and thorough mixing by recycling slurry back into the tank. The circulatory system consisted of a heat transfer section, a cooling section and a pressure drop section. All of the pipe surfaces in contact with the slurry were made of 85 - 15% brass.

The heat transfer section was made of a ½ inch I.P.S. brass pipe inside a 1¼ inch wrought iron pipe which in turn was surrounded by a 2½ inch wrought iron pipe. Steam was circulated through both annular spaces, the outer serving to prevent heat loss from the steam heating the slurry. Iron tees and bushings located at the ends of the 2½ inch and 1¼ inch pipe provided the inlet and outlet for the steam in both annular sections from a common steam header. Sealing of the outer annulus was accomplished by screwing a 2½ x 1½ inch reducing bushing into the 2½ inch tees and inserting the 1¼ inch pipe which was then welded to the bushing. Sealing of the inner annuli was accomplished

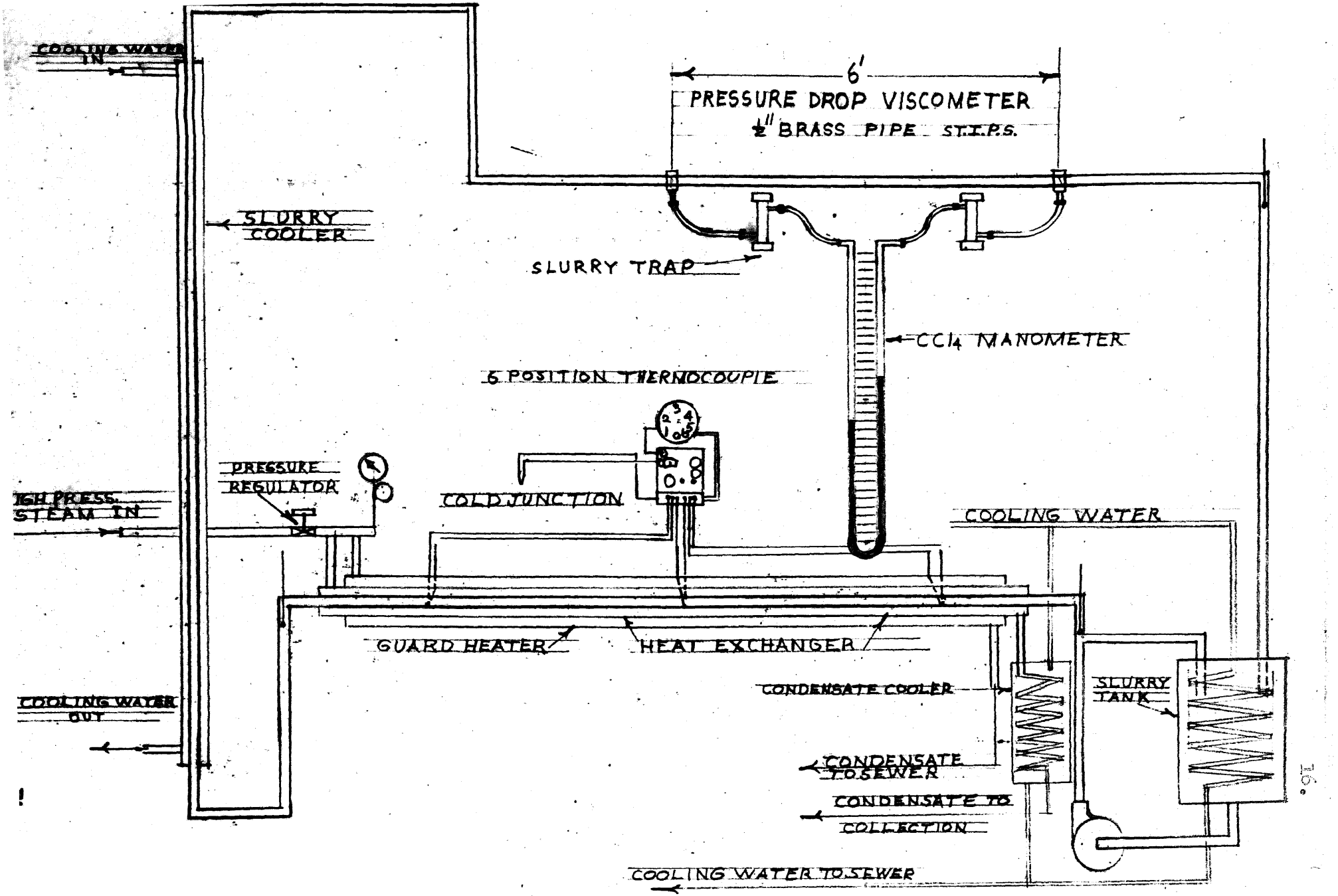
COOLING WATER IN
6'
PRESSURE DROP VISCOMETER
½" BRASS PIPE ST.I.P.S.
SLURRY COOLER
SLURRY TRAP
CCl4 MANOMETER
5 POSITION THERMOCOUPLE
PRESSURE REGULATOR
HIGH PRESS. STEAM IN
COLD JUNCTION
COOLING WATER
GUARD HEATER
HEAT EXCHANGER
CONDENSATE COOLER
SLURRY TANK
COOLING WATER OUT
CONDENSATE TO SEWER
CONDENSATE TO COLLECTION
COOLING WATER TO SEWER

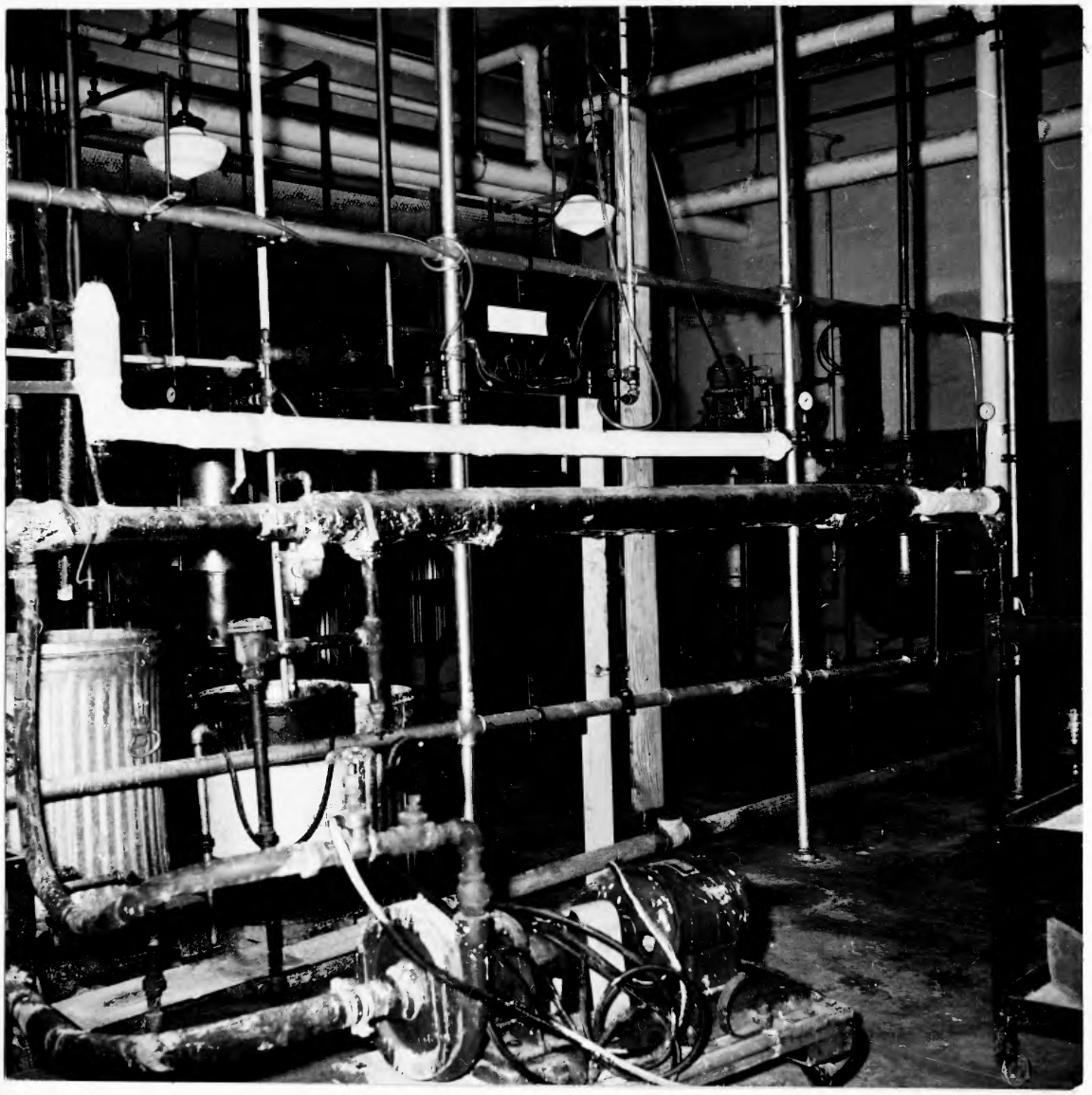

Front View of Apparatus Showing
Heating, Cooling, Pressure Drop, and Calming Sections

Figure 2

Rear View of Apparatus Showing
Slurry, Condensate and Slurry Sample Storage Containers,
Thermocouple Rotary Selector Switch, Potentiometer Platform,
Manometers, and Slurry Traps

Figure 3

with the aid of reducing bushings, close nipples, and unions which were turned down inside and packing added to serve as a packing gland at each end. Air vents were provided at each end of the inner annulus.

Heating of the slurry was accomplished in the ½ inch pipe by steam flowing in the inner annulus counter current to the experimental suspension over a length of 8 feet. Provision was made for collecting and weighing the condensate obtained from the inner annulus. The 12 foot length of the inner ½ inch pipe provided for a calming section of approximately 2 feet at each end. Each end was connected to a 1 inch tee containing a thermometer well in which oil was used as a heat transfer medium. The thermometers used to record the inlet and outlet slurry temperatures were graduated in 1/10°C and ranged from -1° to 101°C. Brass flanges with rubber gaskets were installed between the ends of the ½ inch pipe and the thermometer well tees to minimize end effects due to heat conduction between the heating section and the rest of the apparatus.

Six thermocouples were installed in the surface of the ½ inch brass pipe in the following manner: Three slots or keyways were cut into the pipe wall at either end with the aid of a milling machine. Four of these were made 18 inches long, commencing approximately 12 inches from either end of the ½ inch brass pipe with the two at each end being 180° apart. The third, commencing at the same point as the others on both ends was extended over to the center of the ½ inch pipe with the slot from each end overlapping each other about one half inch at the center and 180° apart. The slots were wide enough to accomodate

a set of copper-constantan thermocouple wires No. 22 gauge. The thermocouple junction was made at the end of each slot and the latter filled with molten solder for the first inch or inch and one half of the end of each slot. The solder was smooth and polished with emery cloth until the surface was uniformly circular. The thermocouple wire was snugly positioned along the length of the slots and litharge cement was used to fill the remaining volume within the slots. The entire pipe surface was polished smooth with fine emery paper. With the thermocouples installed in this manner, they provided temperature measurements at each side of the pipe about six inches from each end of the heating section and at the top and bottom in the middle.

The exposed portion of the wires for the three thermocouples at each end were taped to the ½ inch inner brass pipe and surrounded with individual strands of plastic translucent tubing for protection. This provision was made for the length of wire extending from the ½ inch pipe out to a terminal block adjacent to a rotary selector switch. In addition to the use of a strand of plastic tubing for each set of thermocouple wires, a larger size of plastic tubing was used to contain all three of the individual thermocouples at each end.

The thermocouple wires, contained within the plastic tubing, were connected to a terminal block and from this point connected through a rotary switch to a Leeds Northroup portable precision potentionmeter. An ice bath was used as a reference junction.

The heating section was completely insulated with 85% magnesia pipe insulation and aluminum foil. The cooler was a double pipe type heat exchanger consisting of 1 inch brass I.P.S. pipe inside a 2 inch standard I.P.S. steel pipe. Cold water was circulated countercurrent to the slurry through the annular space. In addition to this, one hundred feet of one-half inch tightly wound copper coil was installed in the slurry tank. Cooling water was passed through the coil to maintain isothermal conditions in the slurry tank. By correctly adjusting the cooling water rate for these two coolers, the temperature of the viscometer was kept close to the average temperature of the heat section.

The viscometer consisted of an insulated $\frac{1}{2}$ inch I.P.S. brass pipe with pressure taps spaced 6 feet apart. A 2 foot long calming section preceded the pressure drop section. Approximately 30 inches beyond the pressure drop section provision was made for a tee containing a thermometer well. A carbon tetrachloride manometer was used to determine pressure drop data. Traps were installed just after the pressure taps to prevent slurry particles from reaching the manometer lines. Lines to and from the traps were made of transparent plastic tubing. This provision enabled viewing air or solid material which occasionally found its way into the manometer lines. The manometer was so built that the traps and transparent lines could be conveniently flushed with water. This was done before all readings to remove sediment and air from the lines and traps.

The pipe returning to the slurry tank was provided with a set

of quick opening valves to conveniently allow diverting the slurry into a weighing tank for flow rate measurements.

The steam condensate was piped from the trap at the end of the inner annulus to a copper coil which was contained in a cooling tank which had water flowing in the bottom and out the top. The end of the copper coil had a flexible hose attached which was used to divert the condensate into a tared receptacle for rate determinations.

EXPERIMENTAL PROCEDURE

The apparatus was first operated with water and the data used to plot Figures 5 and 6. The data for Figure 6 was obtained from the pipe line viscometer and shows excellent agreement with the line obtained from the von Karman equation (14) as shown by the broken line below it. The heat transfer data gave a line with the same slope as the accepted data (13) although the intercept was greater. Four additional water runs were made to check the von Karman plot. For these runs the heat transfer data was not taken. This data agreed well with the first ten runs.

After the water runs had been shown to be acceptable, the slurry runs were started. For each set of runs about forty gallons of water were run into the slurry tank and the pump started to circulate it through the system. The "Lightning" mixer was turned on and sufficient solid was added to give approximately the weight percent of solid desired.

The steam and cooling water to the cooling section, the helical copper coils in the slurry tank, and the condensate cooling tank were then turned on. The slurry rate was set by manipulating the pump discharge valve in conjunction with the by-pass valve to give the approximate desired rate as shown by the pressure drop differential on the manometer in the pipe line viscometer. The system was then allowed to come to steady state as evidenced by constant readings of the inlet and outlet temperatures and the manometer. When steady

state was reached, the thermocouple millivolts, the inlet and outlet slurry temperatures, the viscometer temperature, the manometer differential, and the steam pressure were observed and recorded. The inlet temperature, outlet temperature and manometer differential were averaged over the last two or three readings, if there was a variance, to minimize the effect of small fluctuations. The steam rate was determined by weighing a sample collected over a known period of time. The slurry flow rate was determined by diverting the flow to the slurry tank into a tared tank on a portable platform scale and weighing the contents collected over a known period of time. At least seventy-five pounds of slurry were collected to minimize the error in the determination. A pair of quick opening valves insured rapid change-over from flow to the slurry tank to flow to the tared tank and vice versa.

The density of the suspension was obtained by weighing four liters of the slurry in a flask in which the same volume of water had previously been weighed. This density was in turn used to determine the weight-fraction of solid in the slurry from previously prepared curves based on known concentrations. These curves which are illustrated in Figure 4 were prepared by weighing a clean dry volumetric flask. It was then filled to the graduated mark with water and weighed accurately. The water was poured out and about two grams of solid added and weighed after which the flask was again filled with water leaving the solid in the flask. By subtracting the tare weight of the flask from both the weight of the flask plus the water alone and the weight of the flask plus the water and the solid, the density

was found by dividing the latter by the former. The weight fraction was determined from the weight of the solid and the weight of the solid-water mixture. This procedure was continued with four samples of each solid at steps of two grams, five grams, ten grams and fifteen grams as shown in Table No. II, and a plot of density versus weight fraction was made.

TABLE I

SOURCE OF MATERIALS AND THEIR PHYSICAL PROPERTIES *

Material	Source	Density at 20°C gm/cc	Sp. Heat 60°C BTU/lb°F	Therm. Conduc. BTU/hr°F/ft.	Av. Part. Size Microns
Atomite Chalk Powder	Thompson, Weinman & Co. Montclair, N.J.	2.71 (Co.)	0.209 Perry	0.40 Perry	2.5 (Co.)
Snowflake White Powder	Thompson, Weinman & Co. Montclair, N.J.	2.71 (Co.)	0.209 Perry	0.40 Perry	6 (Co.)
No. 1 White Powder	Thompson, Weinman & Co. Montclair, N.J.	2.71	0.209 Perry	0.40 Perry	14 (Co.)
Copper Powder	Charles Hardy, Inc., New York City. Electrolytic Copper Powder	8.92 Perry	0.0932 Perry	220 Perry	30.0 **

* All Properties of Water from Perry (16)

Thermal Conductivity of Brass (85015 red brass) 90 BTU/Hr°F/ft.

** As calculated from size distribution data supplied by the manufacturer.

TABLE II

DENSITY - WEIGHT PERCENT DATA

Solid	Wt. Solid in 100 cc slurry/gms.	Total Wt. of 100 cc slurry/gms.	Temp.°C	Wt. % Solid	Slurry Density gms/cc.
Atomite	2	100.62	26	1.9	1.007
	5	102.47	26	4.9	1.026
	10	105.72	26	9.5	1.059
	15	109.2	26	13.7	1.094
Snowflake White	2	100.7	25	2	1.008
	5	102.4	25	4.9	1.025
	10	105.7	25	9.4	1.058
	15	108.5	25	14.2	1.086
No. 1 White	2	99.73	25.5	2	.9988
	5	102.63	25.5	4.8	1.028
	10	105.63	25.5	9.4	1.058
	15	108.53	25.5	13.8	1.087
Copper				1.411	1.00
				3.35	1.02
				6.41	1.05
				10.75	1.095
				13.99	1.124

DENSITY – WEIGHT FRACTION CURVES

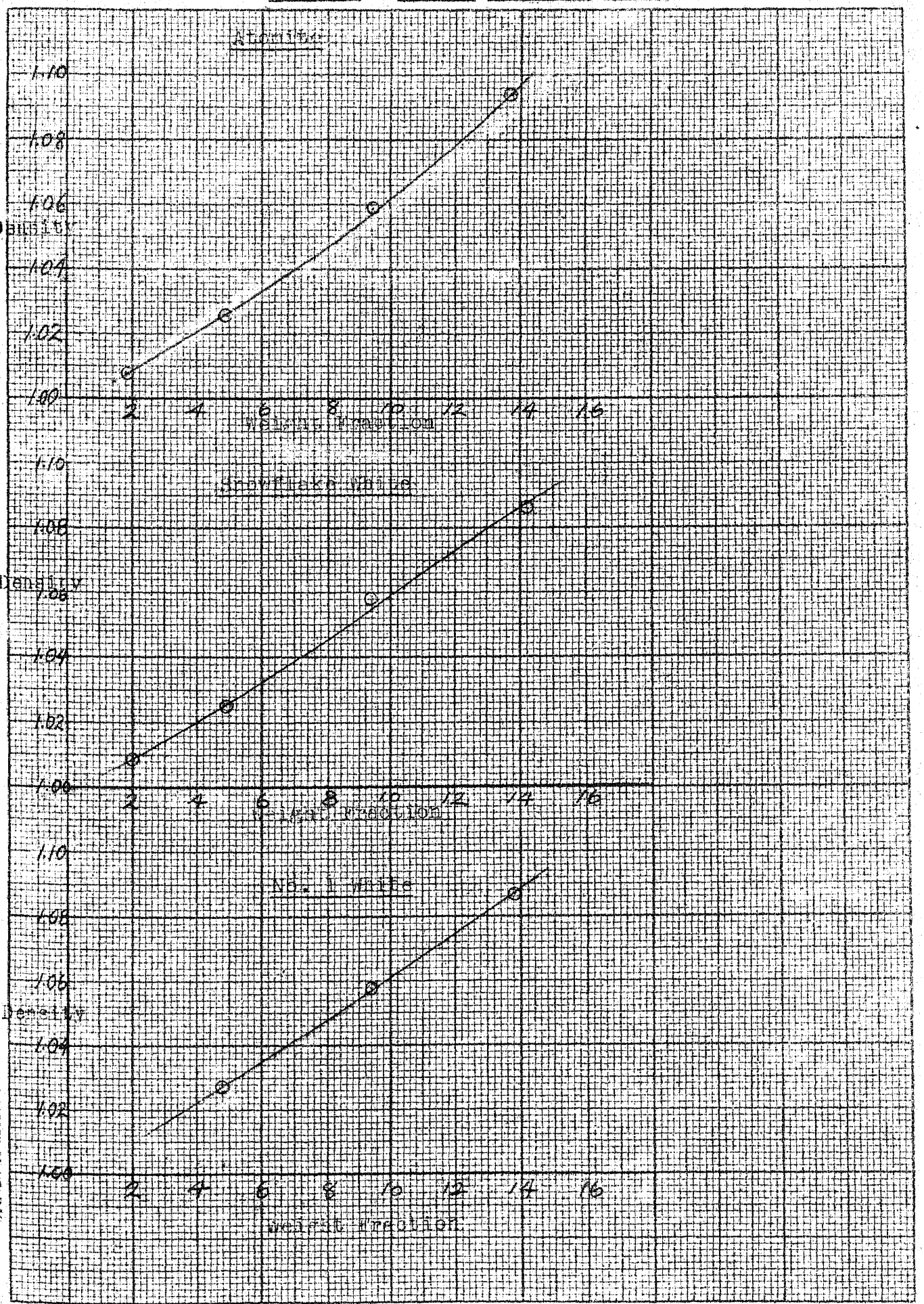

Figure 4

TABLE III OBSERVED DATA WATER CALIBRATION RUNS

Run No.	1	2	3	4	5	6	7	8	9	10	11	12	13	14
Inlet Temperature ^{o}C	33.3	47.7	46.2	44.0	40.8	33.7	31.5	23.6	38.8	43.5				
Outlet Temperature ^{o}C	78.2	75.1	75	76.3	75.5	74.3	76	73.5	78.1	78.1				
Average Temperature ^{o}C	55.8	61.4	60.6	60.2	58.2	54.0	53.8	48.6	58.5	60.8				
T.C.1 mv.	4.55	4.4	4.52	4.5	4.22	4.36	4.41	4.62	4.51	4.6				
T.C.2 mv.	4.34	4.05	4.16	4.1	3.86	4.15	4.28	4.62	4.16	4.05				
T.C.3 mv.	4.15	3.82	3.85	3.9	3.86	4.03	4.11	4.62	4.09	3.94				
T.C.4 mv.	4.45	4.28	4.41	4.39	4.33	4.43	4.39	4.62	4.54	4.44				
T.C.5 mv.	4.67	4.55	4.6	4.58	4.55	4.54	4.55	4.62	4.74	4.67				
T.C.6 mv.	4.36	4.30	4.33	4.39	4.39	4.46	4.45	4.62	4.6	4.56				
Av. Thermocouple Temp. ^{o}F	217.5	212.1	213.3	213.2	209.0	213.9	215.4	225.2	218.2	217.4				
Viscometer Temperature ^{o}C	58.3	64	63	63	59.8	55.1	55	46.2	60.1	62.7	18	19.2	20.8	22
Water Mass Rate lbs./min.	28.75	81	70.5	58.5	49.5	30.75	25.8	12	40.3	53.5	53	38.5	30.13	18.2
Condensate Mass Rate lbs/min.	3.1	4.25	4.25	4	3.72	2.91	2.65	1.46	3.42	3.96				
Manometer Reading in./ccl_4	9.75	62	51.3	37.63	27.75	12.81	9	3.125	19.19	32.06	37.56	21.38	13.63	5.63
Steam Pressure lbs/in^2	7.2	6.5	6.6	7	6.1	6.5	6	7.1	7.6	7.9				

TABLE IV CALCULATED DATA WATER CALIBRATION RUNS

Run No.	1	2	3	4	5	6	7	8	9	10	11	12	13	14
Friction Factor (f)	.0204	.0165	.0180	.0192	.0198	.02[illegible]36	.0235	.0340	.0206	.0196	.0233	.0252	.0263	.0297
$1/\sqrt{f}$	6.96	7.90	7.45	7.20	7.11	6.5[illegible]0	6.51	5.14	6.95	7.14	6.54	6.29	6.17	5.80
$Re\sqrt{f}$	5,220	14,340	12,980	11,080	9,040	5,5[illegible]60	4,760	2,434	7,550	10,100	4,670	3,650	3,040	2,010
Reynolds Number Re (Heat Xcgt)	36,300	111,700	96,600	79,800	64,200	37,[illegible]100	31,000	12,500	52,500	72,100	30,600	23,000	18,800	11,700
Water Viscosity cp.	0.483	0.443	0.445	0.448	0.470	0.[illegible]05	0.507	0.585	0.468	0.453				
Temp. Drop across pipe wall °F	9.2	15.9	15.1	13.4	12.3	8.[illegible]	8.2	4.3	11.3	13.3				
Inside Pipe Wall Temp. °F	208	196	198	200	197	20[illegible]	207	221	207	204				
Log Mean Temp. Diff. °F	68.0	49.5	54.2	54.0	54.0	69.6	71.0	94.4	63.0	56.9				
Water Heat BTU/hr	139,000	240,000	227,000	202,000	186,000	[illegible],000	124,000	64,800	171,000	200,000				
Steam Heat BTU/hr	178,000	244,000	244,000	234,000	218,000	[illegible],000	152,000	83,800	196,000	227,000				
Film Coefficient, BTU/hr.ft^2°F	1,570	3,740	3,220	2,880	2,650	1,[illegible]93	1,346	528	209	270				
Nusselt Number (N)	215	512	441	394	362	[illegible]84	184	72.3	28.6	36.9				
Prandtl Number (P) (Viscometer Section)	3.10	2.84	2.86	2.87	3.02	3.[illegible]24	3.25	3.75	3.01	2.90				
$P^{0.4}$	1.57	1.52	1.52	1.52	1.56	1.[illegible]60	1.60	1.70	1.55	1.53				
$N/P^{0.4}$	137	338	289	258	233	[illegible]23	115	42.6	18.4	24.1				

HEAT TRANSFER DATA FOR WATER

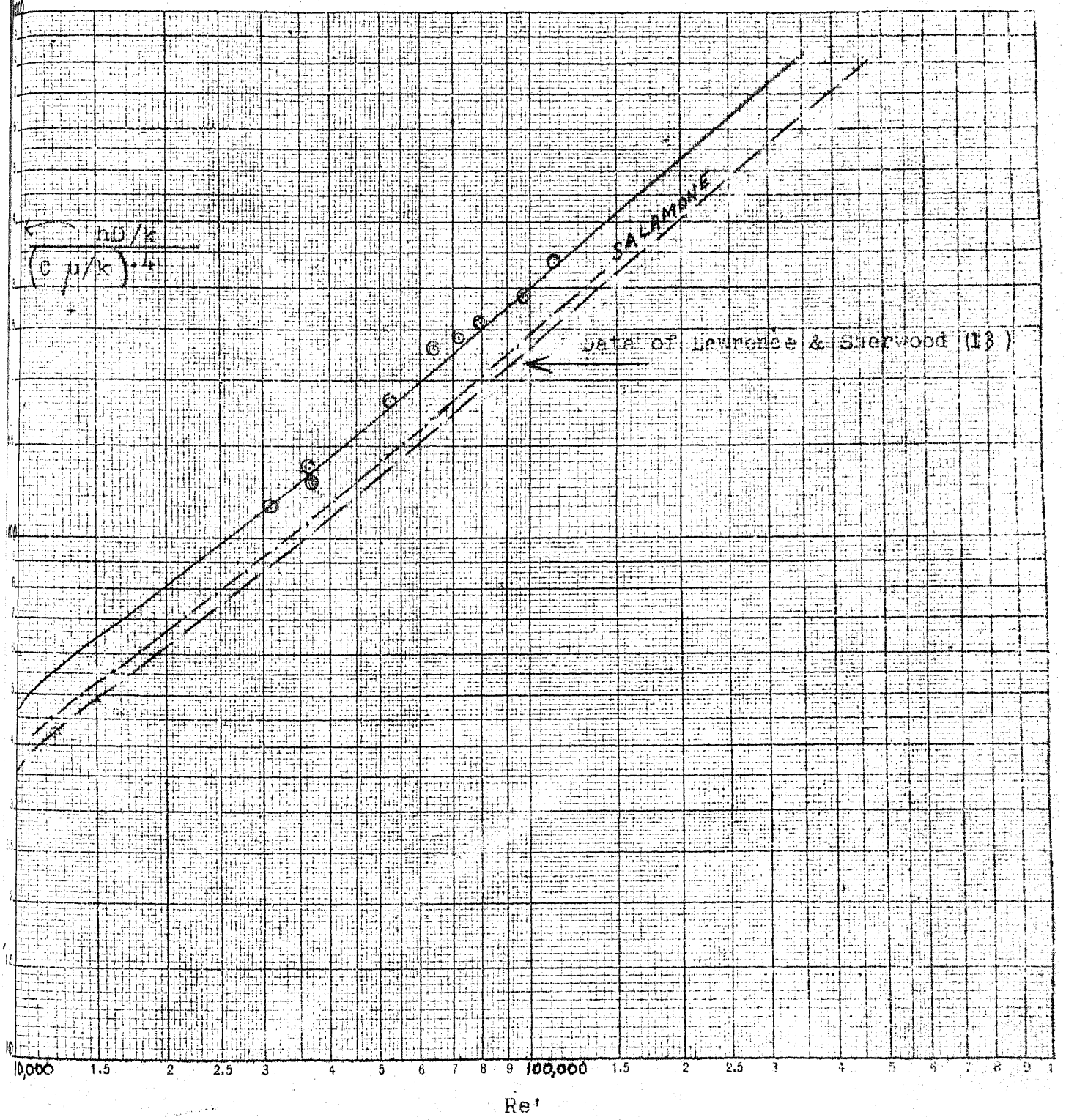

Figure 5

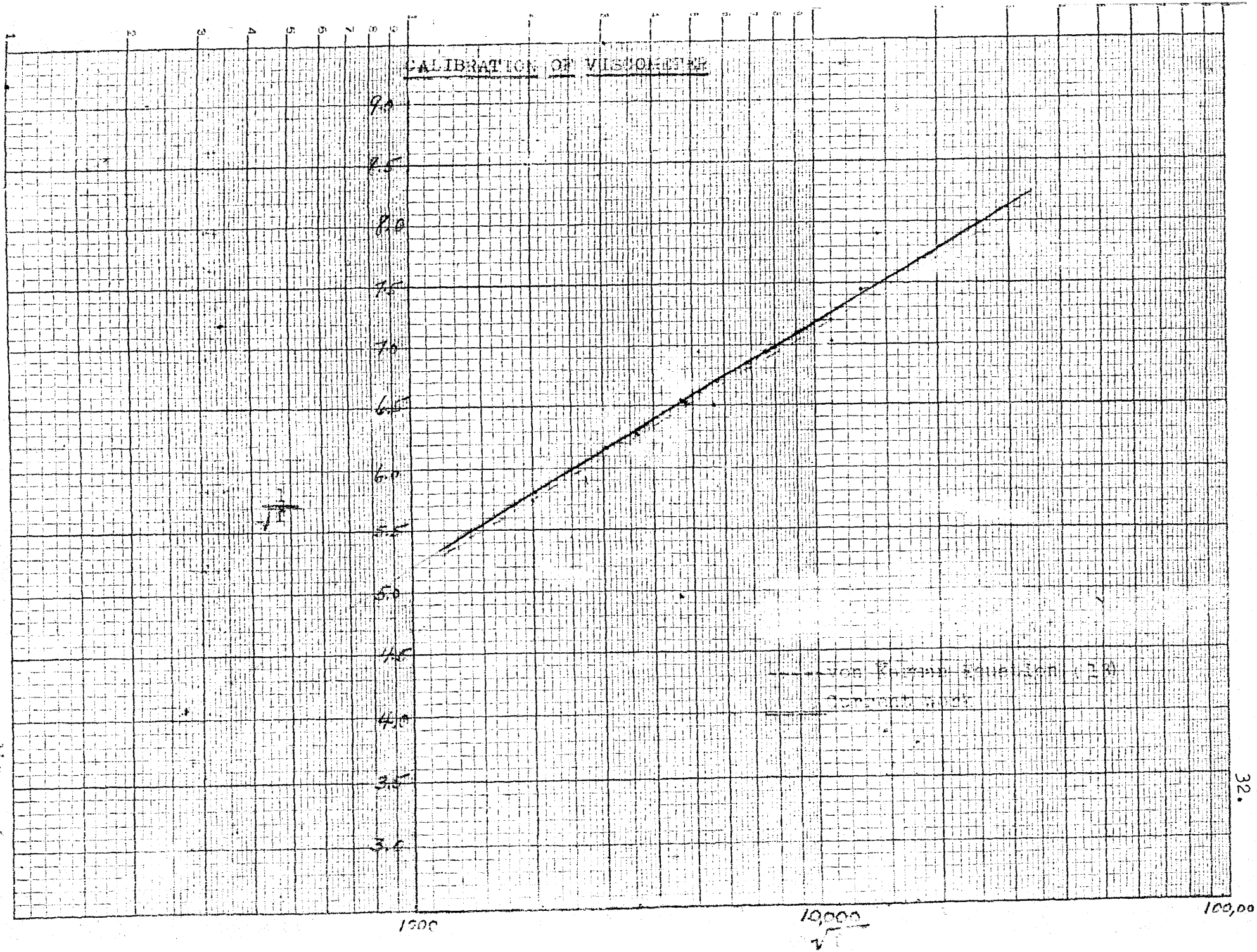
CALIBRATION OF VISIOMETER
9.5
8.5
8.0
7.5
7.0
6.5
6.0
5.5
5.0
4.5
4.0
3.5
3.0
1000
10,000
100,000

TABLE V OBSERVED DATA ATOMITE SLURRY RUNS

Run No.	1	2	3	4	5	6	7	8	9	10	11
Inlet Temperature ^{o}C	38.0	41.0	37.4	32.8	37.0	39.6	41.6	40.1	39.3	38.3	34.2
Outlet Temperature ^{o}C	65.7	67.8	72.5	74.3	70.6	72.1	72.3	74.3	75.8	78.1	80.7
Average Temperature ^{o}C	52.0	54.4	55.0	54.5	54.0	55.8	57.9	58.7	59.6	60.5	59.5
T.C.1 mv.	3.55	3.54	3.81	3.91	3.80	3.72	3.76	3.87	3.93	4.05	4.16
T.C.2 mv.	3.57	3.55	3.81	3.91	3.80	3.76	3.90	4.1	4.00	4.16	4.29
T.C.3 mv.	3.60	3.55	3.73	3.73	3.62	3.65	3.70	3.73	3.75	3.87	4.05
T.C.4 mv.	4.22	4.37	4.38	4.27	4.29	4.31	4.45	4.45	4.45	4.55	4.60
T.C.5 mv.	4.42	4.51	4.59	4.49	4.57	4.65	4.86	4.81	4.81	4.85	4.89
T.C.6 mv.	4.27	4.36	4.47	4.49	4.57	4.65	4.82	4.81	4.74	4.80	4.80
Av.Thermocouple Temp.^{o}F	198.9	200.2	206.4	206.8	205.4	205.8	210.5	212.7	212.1	217.6	219.8
Viscometer Temperature ^{o}C	52.0	54.8	56.0	53.5	53.8	55.8	57.0	57.2	57.6	58.2	57.4
Slurry Mass Rate lbs/min.	47.75	57.60	30.60	23.10	38.60	45.62	51.75	41.25	37.60	31.30	21.25
Condensate Mass Rate lbs/min.	2.77	3.02	2.66	2.06	2.68	2.93	3.16	2.81	2.54	2.36	1.95
Manometer Reading in./CCl_4	28.56	34.63	15.94	8.13	18.63	23.88	31.13	20.88	17.50	13.25	7.75
Steam Pressure lbs/in.^{2}	8.2	10.3	10.6	7.8	9.4	11.3	11.2	10.0	10.2	10.5	9.6
Density lbs/ft.^{3}	64.6	63.9	63.6	63.6	63.5	63.3	65.1	65.2	65.2	65.3	65.4

TABLE VI OBSERVED DATA SNOWFLAKE WHITE SLURRY RUNS

Run No.	1	2	3	4	5	6	7	8	9	10	11	12
Inlet Temperature ^{o}C	45.3	45.3	42.6	42.0	38.8	34.3	33.9	37.4	41.3	43.3	45.5	48.1
Outlet Temperature ^{o}C	76.0	77.2	77.6	80.4	80.2	84.2	81.5	80.7	82.1	79.9	78.4	79.0
Average Temperature ^{o}C	55.6	61.2	60.1	61.2	59.5	59.2	57.7	59.1	61.7	61.6	62.0	63.6
T.C.1 mv.	3.65	3.79	3.81	3.92	4.00	4.22	4.22	4.01	4.07	3.90	3.85	3.85
T.C.2 mv.	3.66	3.77	3.92	4.05	4.07	4.22	4.27	4.07	4.23	4.07	3.93	3.96
T.C.3 mv.	3.58	3.68	3.68	3.84	3.83	4.03	4.02	3.85	3.96	3.88	3.77	3.75
T.C.4 mv.	4.38	4.39	4.40	4.54	4.51	4.52	4.60	4.47	4.65	4.55	4.45	4.48
T.C.5 mv.	4.74	4.75	4.73	4.85	4.73	4.77	4.78	4.74	4.98	4.86	4.81	4.83
T.C.6 mv.	4.61	4.66	4.65	4.74	4.69	4.73	4.73	4.68	4.89	4.76	4.70	4.69
Av. Thermocouple Temp. ^{o}F	205	208	209	214	213	217	218	213	219	214	211	211
Viscometer Temperature ^{o}C	58.5	59.1	59.1	60.0	58.1	57.0	57.2	59.0	62.0	62.0	62.7	64.2
Slurry Mass Rate lbs/min.	56.7	48.5	43.5	35.7	28.6	17.2	20.3	27.7	35.1	42.4	50.6	56.1
Condensate Mass Rate lbs/min.	3.14	2.91	2.79	2.58	2.37	1.85	2.00	2.44	2.87	3.03	3.23	3.36
Manometer Reading in/CCl_4	34.2	27.8	22.1	15.7	10.6	5.1	6.9	10.5	15.4	21.0	28.5	34.0
Steam Pressure lbs/in^2	10.0	9.2	9.8	10.8	9.5	10.2	9.5	9.5	12.5	10.5	9.1	9.6
Density lbs/ft^3	64.0	64.0	64.0	64.0	64.0	64.0	66.3	66.3	66.3	66.3	66.3	66.3

TABLE VII OBSERVED DATA NO.1 WHITE SLURRY RUNS

Run No.	1	2	3	4	5	6	7	8	9	10
Inlet Temperature ^{o}C	44.1	44.0	44.0	41.9	38.1	46.2	41.1	42.2	38.5	36.0
Outlet Temperature ^{o}C	77.7	79.8	80.5	81.1	84.6	78.1	76.4	82.1	83.2	83.0
Average Temperature ^{o}C	60.9	61.9	62.3	61.5	61.4	62.2	58.8	62.2	60.9	59.5
T.C.1 mv.	3.63	3.79	3.77	3.81	4.22	3.79	3.77	3.97	4.10	4.14
T.C.2 mv.	3.68	3.79	3.77	3.86	4.10	3.72	3.77	3.97	4.10	4.14
T.C.3 mv.	3.68	3.73	3.73	3.82	3.96	3.66	3.61	3.90	4.02	4.01
T.C.4 mv.	4.50	4.51	4.49	4.52	4.53	4.45	4.43	4.55	4.65	4.65
T.C.5 mv.	4.84	4.80	4.78	4.77	4.88	4.81	4.76	4.83	4.88	4.85
T.C.6 mv.	4.62	4.70	4.70	4.71	4.79	4.69	4.66	4.75	4.81	4.77
Aver. Thermocouple Temp. ^{o}F	209	210	209	211	217	208	208	214	218	218
Viscometer Temperature ^{o}C	57.6	58.0	58.1	57.5	56.2	59.0	56.5	59.5	58.3	57.0
Slurry Mass Rate lbs/min.	47.6	42.1	39.6	34.0	25.1	54.0	44.3	35.4	26.6	22.8
Condensate Mass Rate lbs/min.	2.77	2.83	2.62	1.99	2.40	3.20	2.83	2.50	2.20	1.97
Manometer Reading in/CCl_4	28.6	22.6	20.5	16.5	9.3	33.5	23.9	15.0	9.69	7.25
Steam Pressure lbs/in^2	9.75	9.90	9.20	8.6	10.1	10.3	9.2	10.4	10.2	9.5
Density lbs/ft^3	64.5	64.5	64.5	64.5	64.5	66.4	66.4	66.4	66.4	66.4

TABLE VIII OBSERVED DATA COPPER SLURRY RUNS

Run No.	1	2	3	4	5	6	7	8	9	10	11	12	13	14	15	16
Inlet Temperature, °C	44.7	44.0	40.5	36.3	38.9	36.2	33.6	46.9	47.3	40.8	44.3	35.5	31.6	43.1	46.0	36.7
Outlet Temperature, °C	77.8	81.4	81.4	82.0	82.9	83.9	83.9	88.9	84.6	92.2	88.1	87.9	87.6	81.7	81.0	85.2
Average Temperature, °C	61.3	62.2	61.0	59.2	60.9	60.1	58.8	67.9	66.0	66.5	66.2	61.7	59.6	62.4	63.5	61.0
T.C. 1 mv.	3.64	3.90	3.93	3.86	3.75	3.95	4.10	3.80	3.60	4.09	3.82	3.63	3.67	3.92	3.78	3.85
T.C. 2 mv.	3.64	3.85	4.86	3.86	3.89	4.10	4.25	4.05	3.82	4.23	4.05	3.75	3.67	3.95	3.81	3.88
T.C. 3 mv.	3.70	3.91	3.95	3.92	3.96	4.06	4.17	4.18	4.00	4.36	4.16	3.84	3.80	4.07	3.90	3.97
T.C. 4 mv.	4.5	4.66	4.66	4.56	4.59	4.73	4.73	4.97	4.76	5.05	4.89	4.50	4.55	4.60	4.45	4.55
T.C. 5 mv.	4.83	4.99	4.92	4.78	4.83	4.90	4.90	5.30	5.12	5.34	5.17	4.77	4.85	4.82	4.66	4.79
T.C. 6 mv.	4.62	4.83	4.81	4.68	4.69	4.80	4.80	5.13	4.93	5.24	5.02	4.63	4.68	4.74	4.56	4.66
Av. Thermocouple Temp. °F	207.0	215.0	214.5	211.5	212.3	217.8	220.3	223.0	215.8	228.1	221.0	222.3	225.5	202.3	208.5	212.0
Viscometer Temp. °C	62.6	64.3	61.9	58.4	61.1	57.0	54.6	64.4	63.0	61.7	63.0	51.0	53.1	60.0	61.3	57.8
Slurry Mass Rate, lbs/min.	59.2	44.8	39.3	29.4	32.2	25.6	19.4	50.6	58.5	31.5	44.8	20.6	16.7	49.3	62.0	28.3
Condensate Mass Rate, lbs/min.	3.29	3.37	3.07	2.58	2.75	2.31	2.07	4.06	4.22	3.43	3.81	2.39	1.93	3.43	3.07	2.69
Manometer Reading in./CCl_4	33.0	27.0	19.0	11.5	15.00	9.5	6.3	32.0	45.0	14.5	25.5	7.25	4.50	33.0	48.0	12.0
Steam Pressure, lbs/in^2	10.0	12.2	10.7	9	9.4	11.8	10.3	19.8	16.0	18.3	17.3	12.5	11.0	9.6	11.3	9.0
Density, lbs/ft^3	63.6	63.6	63.6	63.6	63.6	63.6	63.6	64.5	64.5	64.5	64.5	64.5	64.5	66.0	66.0	66.0

EXPERIMENTAL RESULTS

The heat balances obtained were very poor, the condensate collected showing a higher heat input than the temperature rise of the slurry in almost all of the cases with the poorest agreement occurring at the lower mass rates. All of the heat transfer calculations were based on the temperature rise of the slurry and the average value of the calculated slurry heat capacity. Since there was good agreement between our data and published data of other investigators, it was decided not to stop the experimental work to make modifications of the apparatus to improve its performance. The pilot tube of the steam pressure reducing valve is connected to the low pressure side at the end of the header feeding steam to the heat section. It is possible for condensate to be forced into the pilot tube and make the steam pressure unsteady and unreliable. The pilot tube connection should be moved back from the end of the line and pitched away from the pressure reducing valve so that it drains dry and a steam trap should be installed at the end of the header to keep the steam as dry as possible. It is also recommended that a calorimeter be installed on the inlet steam to determine its quality.

The friction factor was calculated from the equation:

$$f = \frac{(\Delta P)\ (D)\ (2gc)}{(\rho)\ (L)\ (V^2)} \qquad (9)$$

The pressure drop was read from the pipe line viscometer which con-

sisted of two pressure taps six feet apart connected to a carbon tetrachloride manometer. The density was determined by comparing the weight of equal volumes of slurry and water at approximately the same temperature and the velocity was calculated from the mass rate.

The reciprocal of the square root of the friction factor was used in the von Karman equation (Figure 6) to obtain a Reynolds Number from which an apparent viscosity was calculated. The viscosity was calculated from data observed at the temperature in the pipe line viscometer and a correction based on the ratio of the viscosity of water at the heat section temperature to the viscosity of water at the viscometer temperature was applied. In most cases this was a small correction since the temperature in the viscometer was always very close to the average temperature in the heat section. This corrected viscosity was used to find a corrected Reynolds Number.

The film coefficient of heat transfer to the suspension was calculated from the conventional equation:

$$h = q/A\,\Delta tm \qquad (10)$$

where q is the rate of heat transfer evaluated from the product of the slurry temperature rise, the mass rate and the calculated slurry specific heat; A is the inside surface area of the heated pipe, and Δtm is the log mean temperature difference between the arithmetic average inside pipe wall temperature and the inlet and outlet slurry

temperatures.

Using the values calculated on the previous page and constants taken from the literature, the Nusselt Number and Prandtl Number were calculated. These values, plus the ratios of thermal conductivity of the slurry to the thermal conductivity of the water, the heat capacity of the slurry to the heat capacity of the water, and the inside diameter of the pipe to the average slurry particle size which were constant for each slurry concentration, were used to calculate the coordinates of Figures 7, 8, 9 and 10.

Salamone (12) has presented a discussion of the magnitude of the possible error in his work and since the equipment, procedure and slurries investigated are substantially the same, his 10% overall error is applicable to this report. The results were plotted on logarithmic paper in Figures 7 and 8. These plots showed the exponent of the Reynolds Number to be 0.7 and for the Ds/D group to be 0.15. Pollara and Binder redetermined the exponent of the ks/kF group and found it to be close to the original value. Their result was 0.08. The modified equation of Salamone becomes:

$$\frac{hD}{k_f} = 0.346\left(\frac{D v \rho}{\mu'}\right)^{0.7}\left(\frac{C_f \mu'}{k_f}\right)^{0.72}\left(\frac{D_s}{D}\right)^{0.15}\left(\frac{k_s}{k_f}\right)^{0.08}\left(\frac{C_s}{C_f}\right)^{0.35} \qquad (1)$$

Figures 9 and 10 give an overall correlation of the data.

SAMPLE CALCULATIONS

Sample Run - Run No. 10 Snowflake Suspension

Refer to Tables VI and X

1. Slurry Density (ρ) — Weight of water at 60°F required to fill 4 liter volumetric flask is 9.688 lbs.

$$\text{Slurry Density} = 62.4 \frac{10.30}{9.688} = 66.3 \text{ lb/cu.ft.}$$

2. Weight % Solid = $\frac{66.3}{62.4} = 1.062$ gm/cc.

3. Mean Specific Heat (C) = $C_f (1 - X) + C_s X$

C_f = Heat capacity of water BTU/lb.°F

C_s = Heat capacity of solid BTU/lb.°F

X = Weight fraction of solid

$C = 1 (1 - .104) + .209 (.104) = .918$ BTU/lb.°F

4. Flow Rate (w) = 77.5 lbs./1.83 min. = 42.4 lbs./min.

5. Slurry Heat (q) = (w) (c) (Temperature rise)

= (42.4) (.918) (79.9°C-43.3°C) (1.8°F/°C)(60 min/hr)

= 154,000 BTU/hr.

6. Steam Heat (q') — From Steam Tables a plot of vapor Enthalpy minus Liquid Enthalpy vs. Steam Pressure was made and from this the Latent Heat was taken.

q' = (Condensate Rate lb/hr) (Latent Heat BTU/lb)

= (3.03 lb/min) (60 min/hr) (952 BTU/lb)

= 173,000 BTU/hr.

7. Viscometer Friction Factor (f)

$$f = \frac{(\Delta P)\ (D)\ (2gc)}{\rho\ L\ v^2}$$

D = 0.0518 ft. - ID of 1/2" pipe

L = 6.0 ft. - Distance between manometer taps

$$v = \frac{W\ \#/min}{60\ sec/min. \times 66.3\ lbs/ft^3 \times .00211\ ft^2}$$

$$= 0.119\ W$$

$$\Delta P = \frac{21.0\ in}{12\ in/ft} \times 62.4\ lbs/ft^3\ (1.6-1.0) = 65.5\ lbs/ft^2$$

$$f = \frac{(65.5)\ (.0518)\ (2)\ (32.2)}{(66.3)\ (6.0)\ (0.119 \times 42.4)^2} = 0.0216$$

8. Apparent Viscosity (μ_b)

$$1/\sqrt{f} = 1/\sqrt{0.0216} = 6.80$$

From Figure No. 6 $\quad Re\sqrt{f} = 6400$

Reynolds Number (Re) = $6400 / \sqrt{0.0216} = 43,500$

$$\mu_b \text{ (in viscometer)} = \frac{DG}{Re}$$

$$G = \frac{W}{S} = \frac{W}{.00211\ ft^2}$$

$$\mu_b = \frac{(.0518ft)(W\ lbs/min)}{(.00211ft^2)\ (Re)} = 24.5\ \frac{42.4}{43,500} = .0238\ lbs/min.ft$$

Average temp. in Heat Section = 61.6°C

Viscometer Temperature = 62.0

Viscosity of Water at 61.6°C = 0.458 cps

Viscosity of Water at 62.0°C = 0.455 cps

$$\mu_b' \text{ (Corrected to heat section temp)} = \mu_b\ \frac{.458}{.455} = 0.0240\ lbs/ft$$

9. Heat Section Reynolds Number

$$Re' = Re \times \frac{.0238}{.0240} = 43,500 \frac{.0238}{.0240} = 43,100$$

10. Experimental Film Coefficient of Heat Transfer (h)

$h = q/A \Delta t_{LM}$

$q = 154,000$ BTU/hr (See calculation No. 5)

$A = 3.14 \times 0.0518$ ft. $\times$ 8.0 ft. $= 1.3$ ft.^{2} (Inside Heated Area)

Calculation of Δt_{LM}

Average temperature from millivolt readings = 214°F

Temperature drop across pipe wall Δt_m

$$\Delta tm = \frac{(q)\ (\text{pipe thickness})}{(K_{metal})\ (\text{Avg. Area})} = \frac{(154,000 \text{ BTU/hr})(\frac{0.109}{12} \text{ ft})}{(90 \text{ BTU/hr °F ft})(\text{Avg. Area})}$$

$$\text{Avg. Area} = \pi D_{LM} L = (3.14) \frac{(0.840 - 0.622)}{(2.3 \log \frac{(0.840)}{(0.622)} \text{ in})(\frac{1 \text{ ft}}{12 \text{ in}})}(8 \text{ ft})$$

$$= 1.52 \text{ ft.}^2$$

$$\Delta tm = \frac{(154,000)\ (\frac{.109}{12})}{(90)\ (1.52)} = 10.2°F$$

Average Inner Surface Temperature = 214 - 10.2 = 204°F

$$\Delta t_{LM} = \frac{(204 - 110) - (204 - 176)}{2.3 \log \frac{204 - 110}{204 - 176}} = 54.4°F$$

$$h = \frac{154,000 \text{ BTU/hr}}{(1.3 \text{ ft}^2)\ (54.4°F)} = 2180 \text{ BTU/hr.ft.}^2°F$$

11. Nusselt Number (N) = hD/k_f

$$k_f = 0.378 \ \frac{\text{BTU - ft.}}{\text{hr.ft.}^2°F}$$

$$N = \frac{2180 \times 0.0518}{0.378} = 299$$

12. Prandtl Number (P) = $C_f \mu' / k_f$

$$P = \frac{(1.0 \text{ BTU/lb}^\circ\text{F})(0.0240 \text{ lb/min.ft.})(60 \text{ min/hr})}{0.378 \text{ BTU-ft/hr.ft}^2{}^\circ\text{F}}$$

$$= 3.81$$

13. $P^{0.72} = 2.55$

14. $N/P^{0.72} = 299/2.55 = 117$

15. $$\frac{N}{(P^{0.72})\ (Re)^{0.7}} = \frac{117}{(43{,}100)^{0.7}} = 0.630$$

16. $$\frac{\text{Diameter of Pipe}}{\text{Diameter of Particle (Assuming a sphere)}} = \frac{D}{D_s}$$

$$\frac{D}{D_s} = \frac{0.622 \text{ in}}{0.0000397 \text{ in/micron} \times 6 \text{ microns}} = 2.61 \times 10^3$$

C A L C U L A T E D R E S U L T S

TABLE IX CALCULATED DATA ATOMITE SLURRY RUNS

Run No.	1	2	3	4	5	6	7	8	9	10	11
Friction Factor (f)	.0223	.0191	.0303	.0271	.0228	.0206	.0212	.0224	.0226	.0246	.0312
$1/\sqrt{f}$	6.70	7.24	5.75	6.06	6.62	6.96	6.86	6.70	6.65	6.36	5.66
Re $\sqrt{f}$	5,750	10,600	1,850	2,700	5,200	7,800	6.900	5,750	5,400	3,850	1,680
Reynolds Number Re	38,600	76,800	10,600	16,300	34,400	54,100	47,200	38,600	36,000	24,500	9,490
Bulk viscosity μ b lbs/min.ft.	.0303	.0184	.0706	.0348	.0275	.0206	.0268	.0262	.0256	.0313	.0550
Corrected Bulk Viscosity lbs/min.ft. μ'_b cp	.0303	.0185	.0718	.0342	.0275	.0206	.0264	.0255	.0248	.0302	.0531
Corrected Reynolds Number Re'	38,600	76,500	10,400	16,600	34,400	54,100	48,000	39,600	37,200	25,400	9,800
Mass Fraction of Solid in Slurry (X)	.064	.050	.040	.040	.037	.031	.078	.078	.078	.080	.083
Temp. Drop Across Pipe Wall δt_m °F	9.00	10.30	7.40	6.60	9.04	10.40	10.70	9.50	9.24	8.36	6.61
Inside Pipe Wall Temp. t_{s_i} °F	189.9	189.4	199.0	200.2	196.4	195.4	199.8	203.2	202.9	209.2	213.2
Log Mean Temp. Diff. Δt_{l_m} °F	57.9	56.2	63.0	64.7	63.0	57.8	61.3	63.3	61.5	65.8	69.8
Slurry Heat BTU/hr	135,500	162,000	112,000	100,000	136,000	156,000	161,000	143,000	139,000	126,000	99,800
Steam Heat BTU/hr, q'	159,000	173,000	152,000	118,000	153,000	167,000	180,000	160,000	145,000	135,000	111,000
Film Coefficient (h) BTU/hr.ft.^{2}°F	1800	2,220	1,367	1,190	1,660	2,070	2,020	1,734	1,740	1,450	1,100
Nusselt Number N	246	304	187	163	227	284	277	238	238	199	151
Prandtl Number P	4.81	2.94	11.4	5.43	4.36	3.27	4.19	4.05	3.94	4.79	8.43
$P^{.72}$	3.00	2.13	5.50	3.27	2.80	2.28	2.73	2.66	2.61	2.99	4.45
$N/P^{.72}$	82.0	143.0	34.0	49.8	81.1	124.0	101.0	89.5	91.2	66.5	33.9
$Re^{.7}$	1,720	2,770	660	940	1,590	2,160	1,990	1,740	1,660	1,270	650
$N/P^{.72}Re^{.7}$	.0476	.0516	.0515	.0530	.0510	.0574	.0507	.0514	.0549	.0524	.0522 - Av. 0.0521
D/D_s	6,260	6,260	6,260	6,260	6,260	6,260	6,260	6,260	6,260	6,260	6,260

TABLE X CALCULATED DATA SNOWFLAKE WHITE SLURRY RUNS

Run No.	1	2	3	4	5	6	7	8	9	10	11	12
Friction Factor, f	.0192	.0213	.0210	.0222	.0233	.0310	.0308	.0252	.0230	.0216	.0204	.0198
$1/\sqrt{f}$	7.21	6.85	6.90	6.71	6.55	5.68	5.70	6.29	6.60	6.80	7.00	7.11
$Re\sqrt{f}$	10,500	6,600	7,200	5,800	4,800	1,700	1,770	3,550	5,100	6,400	8,200	9,200
Reynolds Number, Re	75,500	46,600	49,600	38,900	31,400	9,650	10,100	22,300	33,600	43,500	57,300	65,200
Bulk Viscosity μ_b, lbs/min.ft.	.0184	.0255	.0215	.0225	.0224	.0436	.0493	.0304	.0256	.0238	.0216	.0211
Corr. Bulk Viscosity, μ'_b, lbs/min.ft.	.0192	.0247	.0212	.0221	.0221	.0421	.0489	.0304	.0256	.0240	.0218	.0214
Corrected Reynolds Number, Re'	72,400	48,100	50,400	40,600	31,800	9,950	10,200	22,300	33,600	43,100	56,800	64,300
Mass Fraction, Solid in Slurry, x	.048	.048	.048	.048	.048	.048	.104	.104	.104	.104	.104	.104
Temp. Drop Across Pipe Wall Δt_w, °F	11.9	11.0	10.6	9.8	9.0	7.0	7.6	9.2	10.8	11.5	12.2	12.7
Inside Pipe Wall Temp. t_{si}, °F	193.1	197.0	198.4	204.2	204.0	210.0	210.4	203.8	208.2	202.5	198.8	198.3
Log Mean Temp. Diff., Δt_{lm}, °F	46.1	49.0	51.1	54.3	57.3	60.1	65.0	57.2	57.4	52.7	49.8	46.6
Slurry Heat, BTU/hr, q	181,000	161,000	158,000	143,000	123,000	8	95,800	119,000	142,000	154,000	165,000	172,000
Steam Heat, BTU/hr., q'	179,000	166,000	159,500	147,500	135,500	1	114,200	139,000	163,300	172,900	184,700	192,000
Film					1,650	1	1,135	1,600	1,900	2,180	2,550	2,840

TABLE XI CALCULATED DATA NO. 1 WHITE SLURRY RUNS

Run No.	1	2	3	4	5	6	7	8	9	10
Friction Factor, f	.0228	.0230	.0236	.0258	.0267	.0214	.0228	.0224	.0256	.0261
$1/\sqrt{f}$	6.62	6.59	6.50	6.22	6.11	6.85	6.62	6.70	6.25	6.22
$Re\sqrt{f}$	5,200	5,000	4,500	3,300	2,600	6,800	5,200	5,800	3,400	3,300
Reynolds Number, Re	34,400	32,600	29,200	20,500	15,950	46,500	34,400	38,900	21,200	20,500
Bulk Viscosity, μ_b, lbs/min.ft	.0339	.0314	.0332	.0406	.0386	.0284	.0316	.0223	.0307	.0272
Corr. Bulk Viscosity, μ'_b, lbs/min.ft.	.0322	.0296	.0311	.0384	.0357	.0271	.0344	.0214	.0294	.0262
Corrected Reynolds Number, Re'	36,200	34,600	31,200	21,700	17,200	48,800	31,600	40,500	22,200	21,300
Mass Fraction, Solid in Slurry, -x	.056	.056	.056	.056	.056	.115	.115	.115	.115	.115
Temp.Drop Across Pipe Wall, Δt_m, °F	11.0	10.3	9.6	9.2	8.0	12.1	10.8	9.5	8.4	7.5
Inside Pipe Wall Temp. t_{si}, °F	198	200	199	202	209	196	197	204	210	211
Log Mean Temp. Diff. Δt_{lm}, °F	50.5	49.6	46.3	51.6	56.7	46.1	53.5	50.5	59.5	62.9
Slurry Heat, BTU/hr., q	165,000	156,000	145,000	138,000	120,000	169,000	154,000	139,000	117,000	105,000
Steam Heat, BTU/hr., q'	158,000	162,000	150,000	114,000	137,000	183,000	162,000	143,000	126,000	113,000
Film Coefficient BTU/hr.ft.^{2} °F, h	2,500	2,420	2,410	2,060	1,630	2,820	2,210	2,120	1,510	1,280
Nusselt Number, N	342	332	330	282	223	386	302	290	207	176
Prandtl Number, P	5.11	4.70	4.94	6.09	5.66	4.30	5.45	3.40	4.66	4.15
$P^{.72}$	3.12	2.95	3.06	3.54	3.36	2.78	3.28	2.35	2.94	2.70
$N/P^{.72}$	110.0	112.0	108.0	79.7	66.4	139.0	92.0	123.0	70.4	65.3
$Re^{.7}$	1,640	1,590	1,470	1,140	964	2,020	1,480	1,770	1,160	1,120
$N/P^{.72}\ Re^{.7}$	.0671	.0705	.0734	.0700	.0688	.0688	.0621	.0694	.0606	.0583 - Av. 0.0691
D/D_s	1,120	1,120	1,120	1,120	1,120	1,120	1,120	1,120	1,120	1,120

TABLE XII CALCULATED DATA COPPER SLURRY RUNS

Run No.	1	2	3	4	5	6	7
Friction Factor, f	.0205	.0234	.0214	.0231	.0254	.0251	.0296
$1/\sqrt{f}$	6.98	6.53	6.83	6.60	6.28	6.32	5.82
$Re\sqrt{f}$	8,000	4,950	6,700	5,100	3,555	3,700	2,040
Reynolds No., Re	55,800	32,400	46,800	33,700	22,300	23,600	11,900
Bulk Viscosity μ_b, lbs/min.ft.	.0233	.0339	.0206	.0214	.0354	.0266	.0401
Corrected Bulk Viscosity, μ'_b	.0240	.0351	.0214	.0211	.0355	.0253	.0378
Corrected Reynolds Number	54,000	31,300	45,100	34,200	22,700	24,800	12,600
Mass Fraction, Solid in Slurry, x	.03	.03	.03	.03	.03	.03	.03
Temp. Drop across pipe wall, Δt_m °F	12.25	11.60	11.21	9.4	9.9	8.55	7.5
Inside Pipe Wall Temp., t_{si}, °F	195.7	203.4	203.3	202.1	202.4	209.2	212.8
Log Mean Temp. Difference, Δt_{lm}, °F	48.2	51.3	53.3	53.6	51.0	59.0	65.0
Slurry Heat, BTU/hr.	184,500	175,000	169,000	142,000	149,200	129,000	103,000
Steam Heat, BTU/hr.	188,000	192,000	175,500	146,000	155,500	132,000	118,400
Film Coefficient, BTU/hr.ft^2°F	2,940	2,630	2,440	2,040	2,250	1,680	1,400
Nusselt Number, N	403	359	334	279	308	230	192
Prandtl Number, P	3.81	5.56	3.38	3.35	5.63	4.02	6.00
$P^{.72}$	2.55	3.33	2.35	2.33	3.35	2.65	3.51
$N/P^{.72}$	158	109	142	120	92	87	54.7
$Re^{.7}$	2,150	1,443	1,858	1,548	1,125	1,224	763
$N/P^{.72}Re^{.7}$	.0735	.0754	.0764	.0776	.0861	.0771	.0717 - Av. 0.0762
D/D_s	520						

TABLE XIII

OBSERVED AND CALCULATED DATA FOR ATOMITE
FROM SALAMONE (12) FOR FIGURES 7 AND 9

Film Coefficient (h)	Nusselt Number (N)	Prandtl Number (P)	$\frac{N}{P^{.72}}$	Reynolds Number (Re)	Ordinate of Figure 7	Run No.
3575	490	3.46	201	143,800	223.0	89
3072	421	3.59	168	119,600	187.0	90
3076	422	3.72	164	109,200	183.0	91
2644	363	4.04	133	83,300	147.8	92
2373	325	4.35	113	66,500	125.5	93
3531	483	4.30	190	117,000	189.0	94
3256	445	4.35	154	105,500	154.5	95
2974	408	4.55	137	87,200	152.8	96
2563	352	4.74	115	70,600	128.0	97
2190	300	5.13	93	53,600	103.2	98
3491	478	4.89	153	105,300	171.0	99
3141	431	5.61	125	92,800	151.0	100
2978	408	5.06	127	82,500	141.5	101
2684	368	5.25	112	69,200	124.5	102
2289	314	5.64	90	53,100	101.0	103
1703	234	6.58	60	31,100	67.0	104

CORRELATION FOR REYNOLDS NUMBER EXPONENT

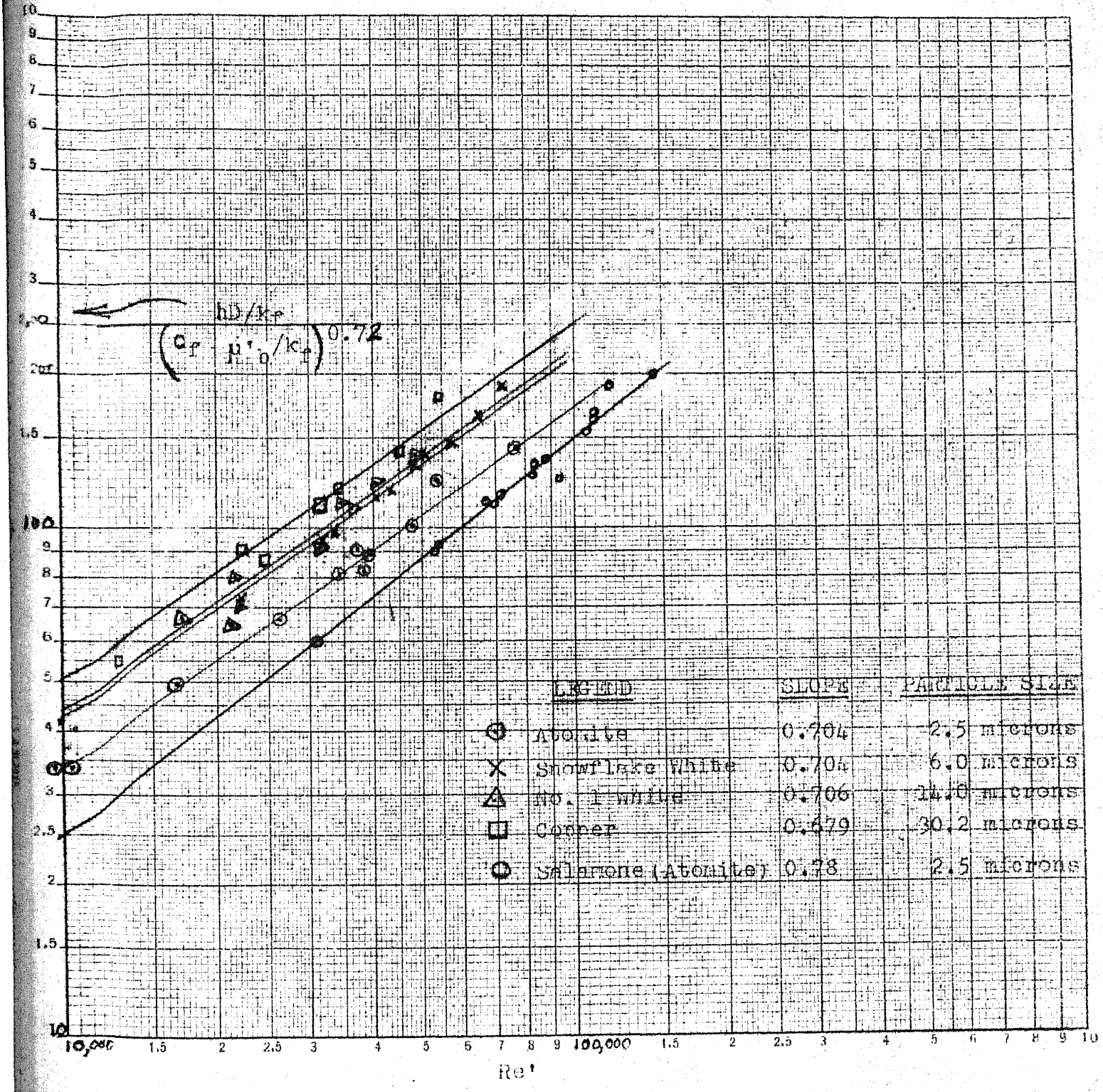

Figure 7

CORRELATION FOR PARTICLE SIZE EXPONENT

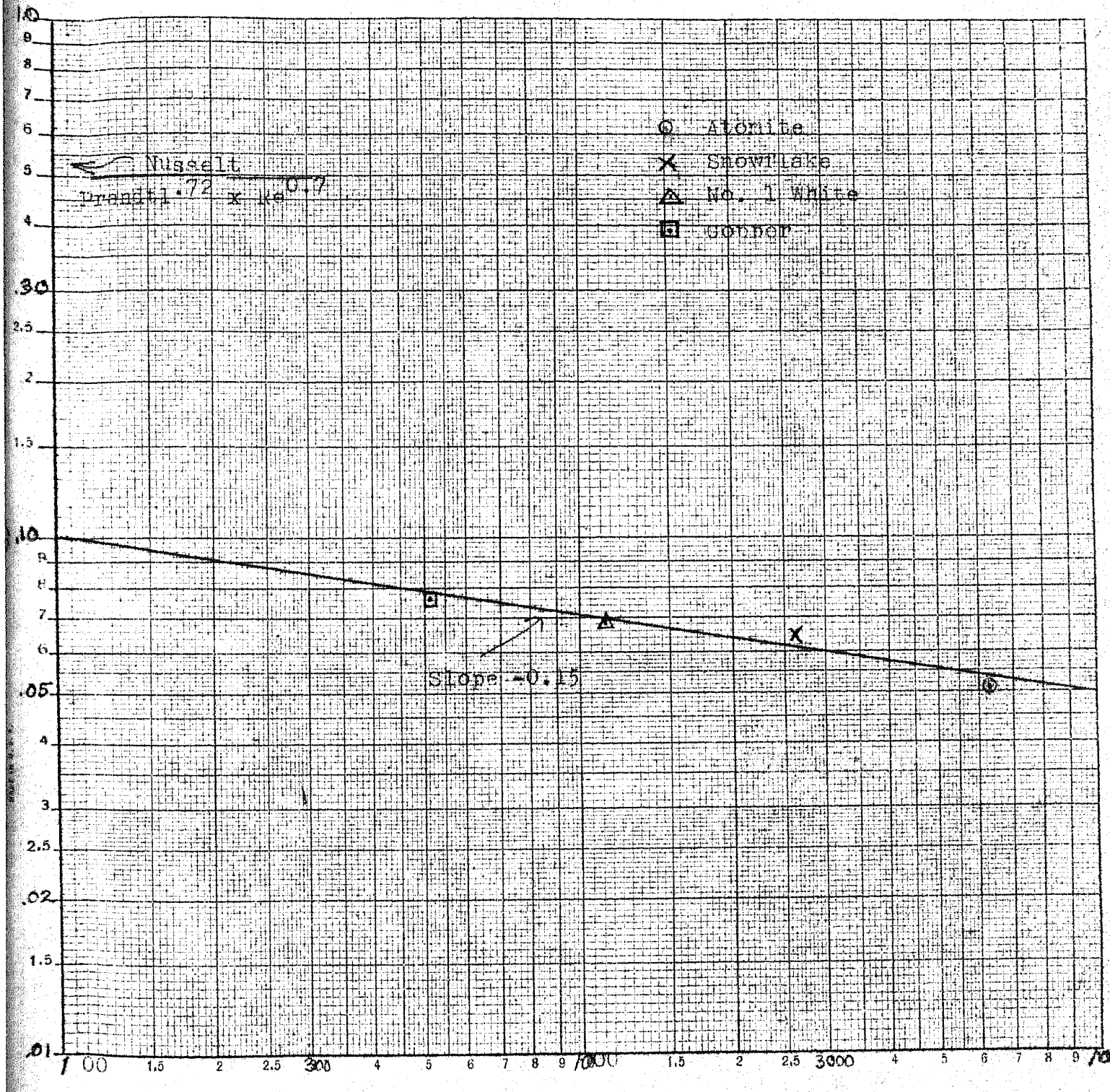

Figure 8

TABLE XIV

CALCULATED RESULTS FOR FINAL CORRELATION DATA FOR COORDINATES OF FIGURES 9 AND 10

Slurry Type	Run No.	Ordinate of Figure 9	Ordinate of Figure 10	Reynolds Number
Atomite	1	90.0	527	38,600
	2	173.0	917	76,500
	3	37.4	219	10,400
	4	54.8	320	16,600
	5	88.6	520	34,400
	6	137.0	800	54,100
	7	111.0	652	48,000
	8	97.5	574	39,600
	9	99.5	585	37,200
	10	74.0	429	25,400
	11	37.4	219	9,800
Snow Flake	1	218.0	1065	72,400
	2	153.0	745	48,100
	3	159.5	780	50,400
	4	133.0	648	40,600
	5	108.0	526	31,800
	6	47.5	232	9,950
	7	42.7	209	10,200
	8	83.6	408	22,300
	9	112.0	549	33,600
	10	139.0	680	43,100
	11	168.0	825	56,800
	12	189.8	928	64,300
No. 1 White	1	131.5	546	36,200
	2	135.0	560	34,800
	3	129.0	536	31,200
	4	95.5	396	21,700
	5	80.5	330	17,200
	6	166.9	690	48,800
	7	110.0	457	31,600
	8	147.3	614	40,500
	9	84.3	350	22,200
	10	78.0	325	21,300
Copper	1	221.0	646	54,000
	2	158.1	384	31,300
	3	190.3	506	45,100
	4	145.2	426	34,200
	5	111.5	327	22,700
	6	105.2	309	24,800
	7	66.4	195	12,600

DATA OF THIS REPORT IN SALADONE CORRELATION

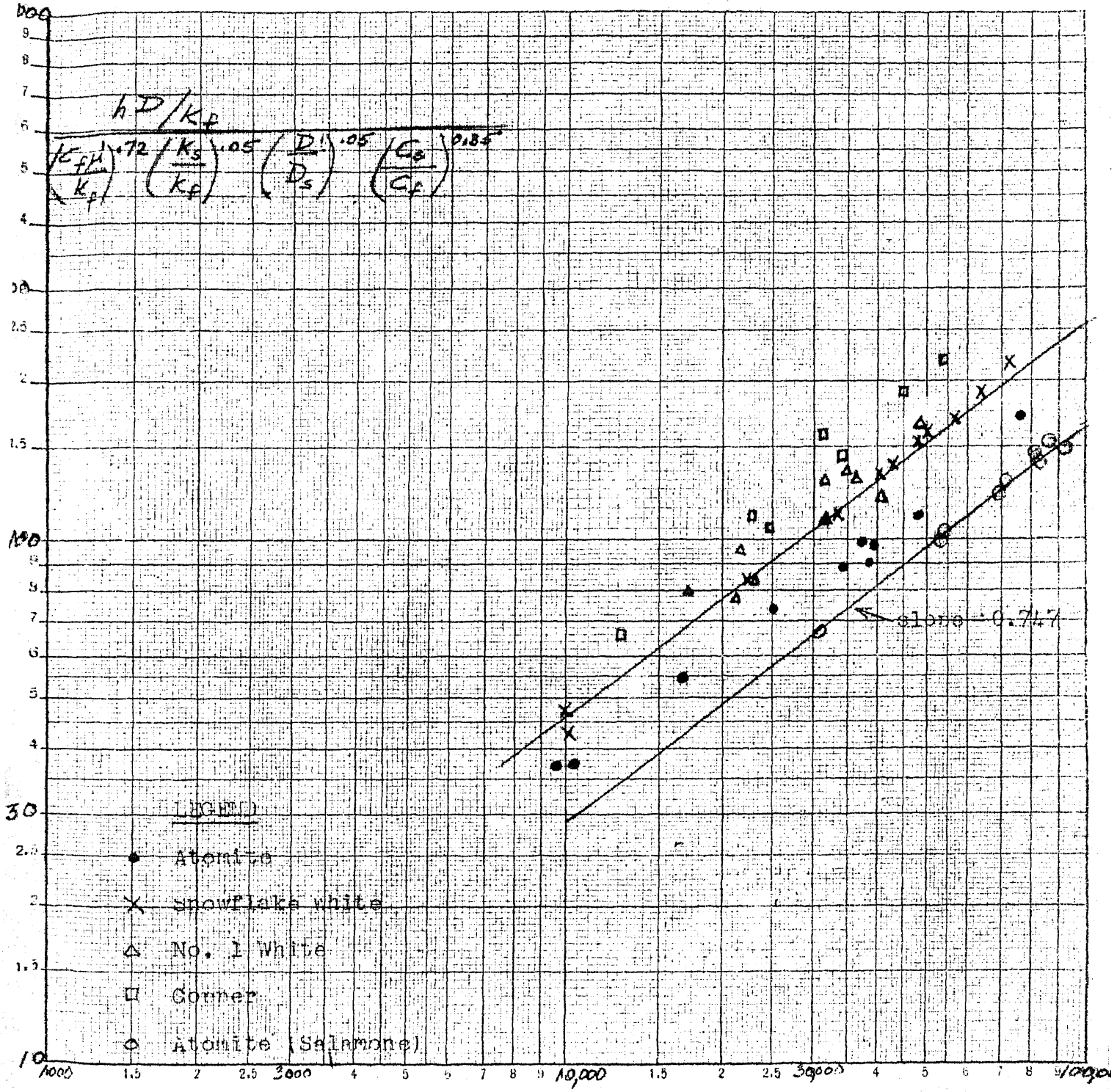

Figure 9

CORRELATION SHOWING DATA OF THIS REPORT

USING EQUATION OF THIS REPORT

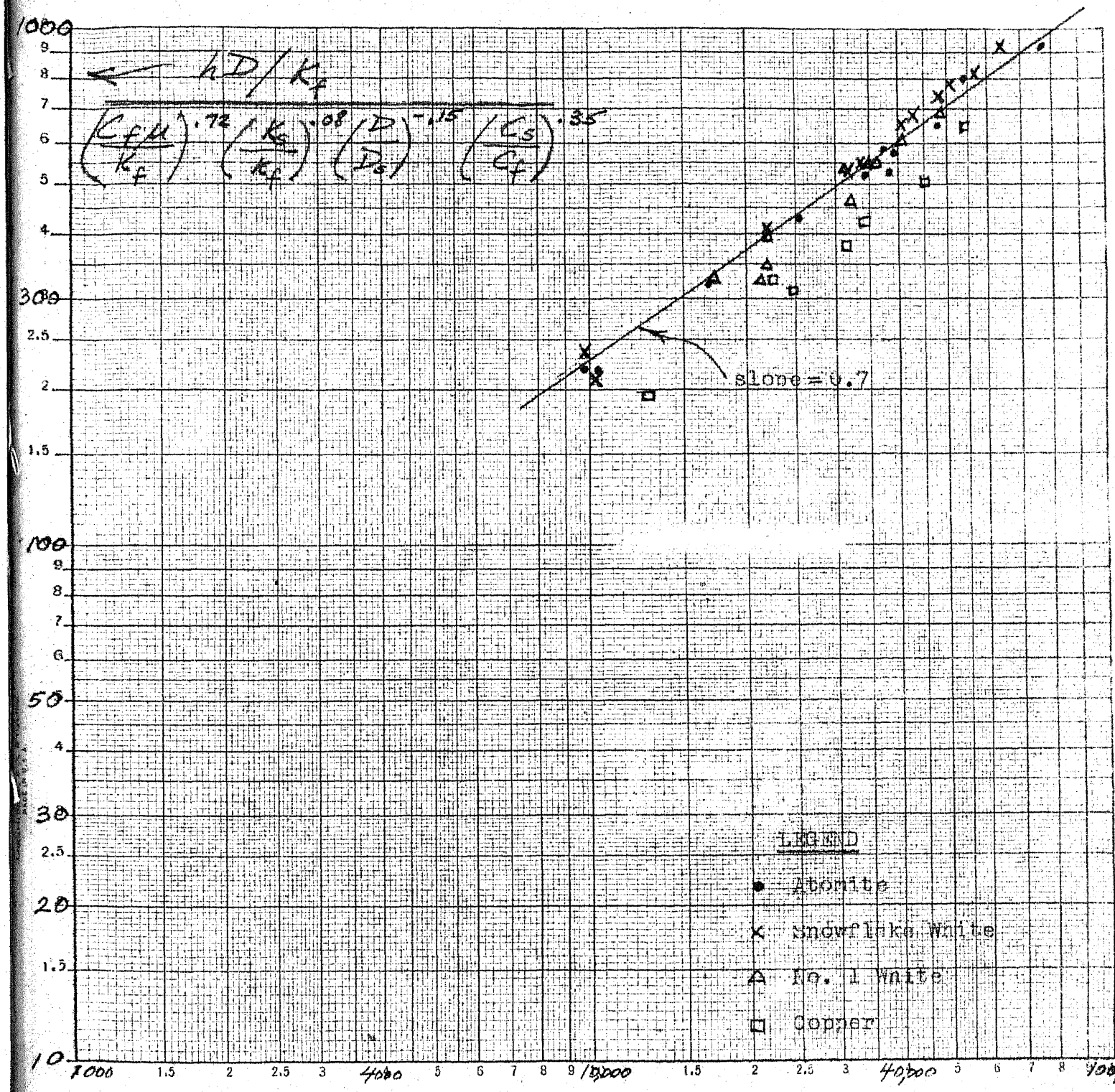

Figure 10

DISCUSSION OF RESULTS

The accepted water data was reproduced satisfactorily in the apparatus calibration runs as shown by Figures 5 and 6. In Figure 5 it will be noted that although the slope of the line produced by the data of this report is the same as that of Lawrence and Sherwood (13) and Salamone (12), the intercept is greater. The same pattern is observed on Figure 6 where the data for the Atomite slurry as obtained from Salamone gives approximately the same slope as the data of this report, but the intercept of the latter is greater. It is suggested that the displacing of these lines to indicate higher actual film coefficients of heat transfer may be due in part to an improved method of installing the thermocouples. They were installed by grooving the outside wall of the pipe parallel to its axis just deep enough so that the thermocouple wire was approximately flush with the pipe wall with only a minimum of protective covering which was smoothed out to match the outside diameter of the pipe. At the end of the groove inside the heating section, the thermocouple junction was embedded in solder as close to the pipe surface as possible. This method of installation should give more accurate measurements of surface temperature than those obtained by Salamone. In addition to this, the thermocouples in Salamone's apparatus were installed by winding them around the outside of the pipe through which the slurry was flowing. It can readily be seen that the temperature of the condensing film on the pipe wall varies from top to bottom as

shown by the fact that thermocouple three installed on the bottom of the slurry conducting pipe always read about 20 - 30 degress less than thermocouple four which was installed on top of the pipe. The thermocouple wires are, therefore, subjected to a more constant heat source since they are in the same position all along the pipe and would not be affected by temperature gradients introducing an error by heat conduction.

The slope of the line in Figure 8 is negative (-0.15) which means that for the slurries under study, the coefficient of heat transfer increased as the particle size increased. This is also shown by Figure 7. Salamone found that the opposite was true at higher Reynolds Numbers with copper slurries ranging in particle size from twenty-one microns to fifty-six microns. It is also interesting to note that the difference in intercept between the Snowflake line (6 microns) and the Atomite line (2.5 microns) is much greater than between the Snowflake line and the No. 1 White line (14 microns). The copper line (30 microns) is higher than the No. 1 White line but here the increment is not so significant since particle size is not the only determining factor in this case. The thermal conductivity of copper is 220 as compared to 0.40 for Calcium Carbonate.

It is suggested that the mechanism may pass through some limiting value or transition period where at lower flow rates heat transfer increases as particle size increases with the magnitude of the

increase in heat transfer for a progression of increasing particle size decreasing until at some limiting value of particle size a further increase in particle size causes a decrease in rate of heat transfer. It is reasonable to assume that if such a transition point exists, that it can be shifted up or down based on the particle size scale by changing the flow rate and, therefore, the turbulence. As long as a high degree of turbulence exists, it will overcome the tendency of the particles to settle and will keep them in motion so that they will contact each other and the hot pipe wall frequently. When a low degree of turbulence exists, these contacts are reduced and the heat transferred by conduction is decreased. The effect of particle size over a range of particle densities is an investigation which may improve the accuracy of this correlation.

The shape of the particles, which in this correlation was assumed to be spherical, may have a significant effect upon the correlation. The shape of the particle will influence its turbulence in suspension and its contact with the heat exchange surfaces. The shape will also effect the surface tension of the dispersing media.

For practical usage, it would be better if it could be determined that the effect of particle shape was not significant since this is a physical property which is difficult tc determine.

Figure 10 shows the data of this report using the modified form of the Salamone equation (Equation 1) as determined as a result of this work and Figure 9 shows the same data using the Salamone equation.

The data correlates better using the modified equation but it is interesting to note that Salamone's data correlates very well with his equation as shown in Figure 9.

SUMMARY AND CONCLUSIONS

New exponents for the Reynolds Number ($DV\rho/\mu$), the thermal conductivity expression (K_s/K_f), and the particle size expression (D/D_s) were developed which, when used with the equation of Salamone:

$$\frac{hD}{k_f} = .131\left(\frac{Dr\rho}{\mu'}\right)^{0.62}\left(\frac{C_f\mu'}{k_f}\right)^{0.72}\left(\frac{D}{D_s}\right)^{0.05}\left(\frac{C_s}{C_f}\right)^{0.35}\left(\frac{K_s}{k_f}\right)^{0.05}$$

resulted in a new equation:

$$\frac{hD}{k_f} = 0.346\left(\frac{Dr\rho}{\mu'}\right)^{0.7}\left(\frac{C_f\mu'}{k_f}\right)^{0.72}\left(\frac{D_s}{D}\right)^{0.15}\left(\frac{C_s}{C_f}\right)^{0.35}\left(\frac{k_s}{k_f}\right)^{0.08}$$

This new equation gave much better agreement with the data collected than the equation of Salamone.

The most significant difference in the two equations is the exponent of the particle size expression. The data indicates that the change in particle size is not directly proportional to the change in the heat transfer coefficient. There seems to be a transition point or limiting value for any solid of given density where the heat transfer coefficient stops increasing as the particle size increases. As the particle size is increased further, the heat transfer coefficient decreases. The data of this report also indicates that this limiting value was approached in larger increments when the particle size was changed from 2.5 microns to 6.0 microns than when it was changed from 6.0 microns to 14.0 microns.

Before any rigorous conclusions can be made on the effect of particle size, it will be necessary to collect more data on more solids in suspension.

The change in the exponent of the thermal conductivity expression has a relatively small effect on the magnitude of the heat transfer coefficients except for solids of very high thermal conductivity.

The change in the Reynolds Number exponent, although it is a minor one, is significant since the Reynolds Number expression is the controlling one in the equation.

UNITS

A = heat transfer surface, $ft.^2$

C_f = specific heat of fluid or suspending medium, $BTU/(lb_m)\ (^oF)$

C_s = specific heat of suspended solid, $BTU/(lb_m)\ (^oF)$

D = pipe diameter, ft.

D_s = average diameter of suspended solid particles, ft.

f = friction factor, dimensionless

g_c = dimensional constant, 32.2 (lb_m) (ft)/(lb_f) $(sec)^2$

h = film coefficient of heat transfer, BTU/hr. ft. ^{2o}F

k_F = thermal conductivity of fluid or suspending medium, BTU^{ft}/hr. ft.^{2o}F

k_s = thermal conductivity of suspended solid, BTU^{ft}/hr. ft.^{2o}F

L = length of pipe, ft., any linear dimension

ΔP = pressure drop in pipe length

q = heat transfer rate, BTU/hr

t = temperature

Δt_{Lm} = logarithmic mean temperature difference between average inside pipe surface temperature and inlet and outlet slurry temperature, ^oF

v = linear velocity, ft/sec.

v_b = linear velocity of suspension based upon bulk density of the suspension, ft/sec.

x = weight fraction of solid

N = Nusselt Number, $\frac{hD}{k}$ dimensionless

P = Prandtl Number, C /k, dimensionless

Re = Reynolds Number, Dv / dimensionless

Re' = Corrected Reynolds Number

ϕ = volume fraction of solid in suspension

ρ_f = fluid density, lb_m/ft^3

μ_f = viscosity of fluid

μ_b = apparent bulk viscosity of suspension

μ' = corrected bulk viscosity

REFERENCES

(1) Wilhelm, R.H., and Wroughten, D.M., Ind. Eng. Chem., 31, 482 (1939).

(2) American Inst. of Physics, "Temperature, Its Measurement and Control in Science and Industry", 855-861, Rheinhold Publ. Corp., New York, (1941).

(3) Wilhelm, R.H., Wroughten, D.M., and Loeffel, W.F., Ind. Eng. Chem., 31, 622, (1939).

(4) Babbit, H.E., and Caldwell, D.H., Ind. Eng. Chem., 33, 249, (1941).

(5) Bingham, E.C., "Fluidity & Plasticity", McGraw-Hill Book Co., Inc., New York, (1922).

(6) Binder, R.C., and Busher, J.E., (Tr. A.S.M.E.), J. of App. Mech., 13, No. 2, A 101, (1946).

(7) Winding, C.C., Baumann, G.P., and Kranich, W.L., Chem. Eng. Prog., 43, 527, 613, (1947).

(8) MacLaren, D.D., and Stairs, R.G., Master's Thesis in Chemical Engineering, Columbia University, (1948).

(9) Alves, G.E., Chem. Engrg., 56, No. 5, 107, (1949).

(10) Shandling, J., Master's Thesis in Chemical Engineering, New York University, (1949).

(11) Hoopes, J.W., et al., Ch. E. S-111 Report, Columbia University, (1945).

(12) Salamone, J.J., Doctor of Engineering Science Thesis, New York University, (April, 1954).

(13) McAdams, W.H., "Heat Transmission", 2nd Ed., Chapt. VII, McGraw Hill Book Co., New York, (1942).

(14) Brown, G.G., and Associates, "Unit Operations", Chapter 12, John Wiley and Sons, Inc., New York, (1950).

(15) Bonilla, C.F., et al., "Preprints of Symposium on Heat Transfer", 44th Annual Meeting A. I. Ch. E., Dec., (1951).

(16) Perry, J.H., (Editor), "Chemical Engineers Handbook", McGraw-Hill Book Co., Inc., New York, (1950).

(17) Orr, C., Jr., and Dalla Valle, J.M., Preprint No. 13, Heat Transfer Symposium, Annual Meeting, A. I. Ch. E., Dec., (1953).

(18) Chu, J.C., Brown, F., and Burridge, K.G., Ind. Eng. Chem., 45, 1606, (1953).